

AnyECG: Evolved ECG Foundation Model for Holistic Health Profiling

Jun Li^{1,2,✉}, Hongling Zhu^{5,✉}, Yujie Xiao^{1,2,✉}, Qinghao Zhao^{6,✉}, Yalei Ke^{7,8,9}, Gongzheng Tang^{1,2}, Guangkun Nie^{1,2,10}, Deyun Zhang¹¹, Jin Li¹², Canqing Yu^{7,8,9}, and Shenda Hong^{1,2,3,4,*✉}

¹National Institute of Health Data Science, Peking University, Beijing, China

²Institute of Medical Technology, Health Science Center of Peking University, Beijing, China

³Institute for Artificial Intelligence, Peking University, Beijing, China

⁴NHC Key Laboratory of Cardiovascular Molecular Biology and Regulatory Peptides, Peking University, Beijing, China

⁵Division of Cardiology, Department of Internal Medicine, Tongji Hospital, Tongji Medical College, Huazhong University of Science and Technology, Wuhan, Hubei, China

⁶Department of Cardiology, Peking University People's Hospital, Beijing, China

⁷Department of Epidemiology and Biostatistics, School of Public Health, Peking University, Beijing, China

⁸Peking University Center for Public Health and Epidemic Preparedness & Response, Beijing, China

⁹Key Laboratory of Epidemiology of Major Diseases (Peking University), Ministry of Education, Beijing, China

¹⁰School of Intelligence Science and Technology, Peking University, Beijing, China

¹¹HeartVoice Medical Technology, Hefei, China

¹²Division of Cardiology, Department of Internal Medicine, Tongji Hospital, Tongji Medical College, Huazhong University of Science and Technology, Wuhan, Hubei, China

#These authors contributed equally

*Correspondence: hongshenda@pku.edu.cn

ABSTRACT

Background: Artificial intelligence-based electrocardiography (AI-ECG) has been proven to detect a variety of cardiac and non-cardiac pathological changes. However, current mainstream research remains limited to independent models for identifying single diseases. These models insufficiently address complex clinical comorbidities and rarely incorporate predictions of future disease risk. Although our previous work, ECGFounder, has achieved coverage of 150 cardiac diseases and significantly improved model performance through fine-tuning techniques, further breakthroughs and expansions are still needed to address key clinical needs and achieve holistic health profiling such as more comprehensive disease screening, long-term risk prediction, and in-depth comorbidity pattern recognition.

Methods: In this study, we constructed a large-scale, multicenter electrocardiogram (ECG) dataset containing 13,348,593 ECG records and their corresponding ICD diagnostic codes from 2,984,209 patients. This dataset integrates retrospective and prospective data, providing a data foundation for multiple tasks including current disease diagnosis, future risk prediction, and comorbidity identification. Methodologically, we employed a transfer learning strategy to fine-tune the pre-trained ECGFounder, successfully developing an improved ECG foundation model, AnyECG, aimed at significantly enhancing its capabilities in holistic health profiling. Furthermore, we conducted extensive multicenter external validation and comprehensively evaluated the model's robustness and accuracy in current diagnosis, future prediction, and comorbidity identification in a 10-year longitudinal cohort study.

Results: We explored the systemic prediction ability of AnyECG across 1,172 ICD-coded conditions. AnyECG achieved an AUROC above 0.7 for 306 of these diseases. The AnyECG model reveals many novel discoveries that have never been reported, demonstrates robust

detection of comorbidity patterns, and shows predictive capability for diseases that may emerge in the future. For example, AnyECG achieved surprising diagnostic abilities for hyperparathyroidism (AUROC: 0.941 [95% CI: 0.903–0.977]), type 2 diabetes mellitus (AUROC: 0.803 [95% CI: 0.798–0.807]), Crohn's disease (AUROC: 0.817 [95% CI: 0.774–0.857]), lymphoid leukemia (AUROC: 0.856 [95% CI: 0.849–0.861]) and chronic obstructive pulmonary disease (AUROC: 0.773 [95% CI: 0.759–0.786]).

Conclusion: This study introduces AnyECG, a new foundation model, and provides substantial empirical evidence for the clinical application of AI-ECG in both current disease detection and future disease prediction, highlighting its potential as a systemic diagnostic tool.

KEYWORDS

ECG, Foundation Model, Disease Profiling

INTRODUCTION

Electrocardiogram (ECG) is a non-invasive, cost-effective, and widely available tool traditionally used to assess cardiac electrical activity^{1,2}. Abnormalities in electrical cardiac activity affect millions of people worldwide and are increasingly recognized as indicators and contributing factors for various health conditions³. It is worth noting that subtle changes in ECG signals often precede the clinical onset of diseases, including arrhythmias, heart failure, and ischemic heart disease^{4–6}. These associations highlight the central role of cardiac electrophysiological homeostasis in maintaining overall health and underscore the potential of ECG for early prediction of a wide range of diseases^{2,7}. However, most existing studies rely solely on isolated ECG indicators (such as QT interval or ST-segment deviations) to establish their associations with specific diseases^{8,9}, while the complex physiological information embedded in ECG signals has yet to be fully explored and integrated for analysis.¹⁰

In recent years, the integration of artificial intelligence (AI) with ECG—termed AI-enhanced ECG (AI-ECG)—has demonstrated significant potential in diagnosing and predicting various diseases beyond arrhythmias, including heart failure, chronic kidney disease, and diabetes^{11–14}. While these efforts represent substantial progress, they face several critical limitations^{15,16}. Most methods target specific diseases or limited disease categories and are constrained by relatively small datasets¹⁷. Furthermore, existing models lack large-scale multi-center external validation, limiting their generalizability to real-world clinical settings^{18,19}. Additionally, most studies focus solely on diagnosis and do not conduct longitudinal cohort-based prediction and risk assessment. Moreover, prior research has not systematically explored the scientific discoveries underlying ECG's ability to diagnose and predict diseases²⁰.

Foundation models offer a promising solution to address these challenges through transfer learning. In the biomedical field, foundation models have exhibited remarkable capabilities across multiple medical domains, advancing disease prediction, diagnosis, and therapeutic discovery^{21,22}. Recently, several ECG foundation models have been proposed^{23–25}. ECG-FM was pre-trained using self-supervised learning on two large ECG datasets²³. CREMA was designed to learn generalizable representations through self-supervised pretraining on 1 million ECGs dataset.²⁴ Despite achieving commendable results, these studies on ECG foundation models narrowly focus on arrhythmia- and cardiac-specific outcomes, restricting the broader potential of foundation models in disease prediction. In our earlier research, we developed ECGFounder using a supervised learning paradigm, based on the largest current ECG dataset—the Harvard-Emory ECG Database (HEEDB)^{25,26}. This dataset included 10,771,552 ECGs from 1,818,247 patients.

While ECGFounder performed well on several downstream tasks, establishing the feasibility of our AI-ECG foundational model, its core capabilities remain primarily focused on arrhythmia detection. Further research is needed to explore how to leverage ECG for screening non-cardiac systemic diseases, predicting future health risks, and identifying comorbidity patterns—i.e., constructing holistic health profiling.

In this study, we systematically explored the role of cardiac electrical activity in disease diagnosis and risk prediction both in cardiac or non-cardiac diseases. We fine-tuned a pre-trained ECGFounder model based on large-scale paired ECG–ICD data to enhance its ability to identify multiple disease spectrums, and performed external validation in multi-center independent cohorts. To further examine the model’s cross-population and cross-regional generalization performance, we also conducted additional validation in the China Kadoorie Biobank (CKB)²⁷. Overall, this study constructed a large-scale, multicenter, multinational ECG cohort covering 2,984,209 patients and 13,348,593 ECGs, including both retrospective and prospective data, providing a data foundation for creating holistic health profiles of patients.

This approach enables the model to align with various diseases and clinical events, ultimately developing AnyECG, a versatile model designed to predict over 800 disease types. Through extensive multi-center validation, we aim to demonstrate that AnyECG can (1) diagnose a wide spectrum of diseases, (2) analyze comorbidity relationships, and (3) perform effective disease screening (Figure 1b). Furthermore, we explored the correlations among different diseases within the ECG framework. By identifying association patterns across various disease systems, we hope to contribute to the understanding of disease mechanisms and potentially uncover new insights into disease interactions.

Our objective was to further enhance ECGFounder using paired ECG and ICD diagnosis data, and to develop a unified model, AnyECG, covering the full spectrum of 1,172 diseases. With this model, we reported previously unrecognized disease associations detectable from ECGs, demonstrated its ability to reveal links between comorbidities, and showed its potential for predicting future disease onset. In this way, we extend the role of the ECG from a cardiac-centered tool to a comprehensive platform for current disease detection and future disease prediction.

Methods

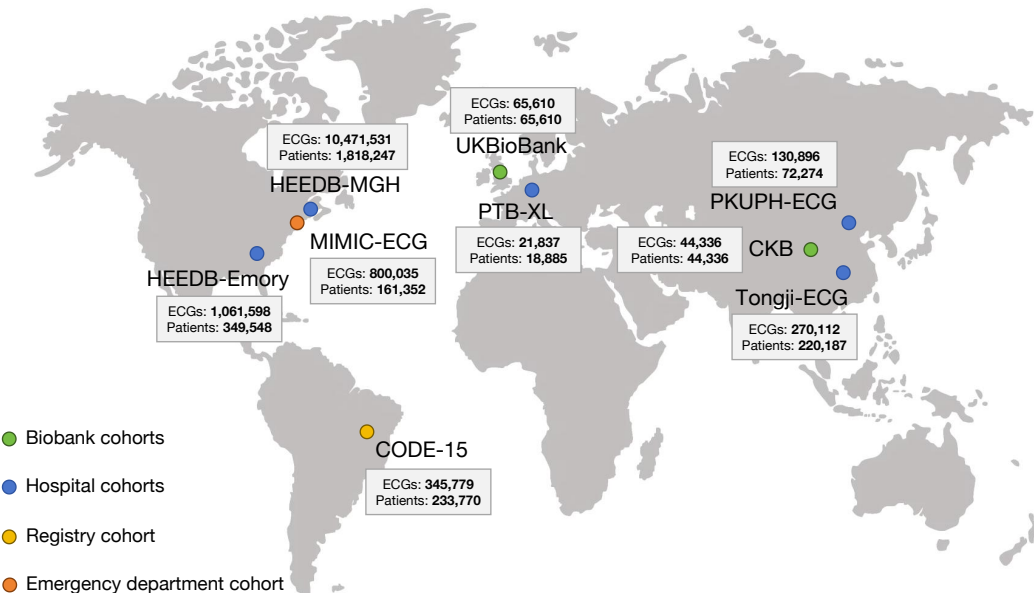
Datasets

We utilized nine large-scale ECG Datasets, MGH-ECG Dataset²⁶, Emory-ECG Dataset²⁶, PTB-XL²⁸, CODE-15²⁹, MIMIC-ECG³⁰, and Huazhong University of Science & Technology Tongji Hospital Dataset (Tongji-ECG) for model development, and Peking University People’s Hospital ECG Dataset (PKUPH-ECG), UKBB-ECG³¹ together with the China Kadoorie Biobank ECG Dataset (CKB-ECG) for external validation²⁷.

HEEDB-MGH Dataset The HEEDB-MGH Dataset is a large-scale, retrospective collection of 12-lead ECGs acquired in routine clinical care, developed through collaboration between Harvard University and Emory University²⁶. It contains 10,608,417 ECG records from 1,818,247 patients at Massachusetts General Hospital (MGH), spanning several decades from the 1990s onwards. Records are sampled at either 250 Hz or 500 Hz, each with a duration of 10 seconds, and stored in WFDB format. Annotations generated by the 12SL-ECG analysis program are available for 10,471,531 MGH records, covering diagnostic statements, ECG morphology, and rhythm patterns. The dataset provides temporal and demographic diversity, making it a valuable resource for large-scale studies on cardiac diseases, arrhythmia prediction, and other ECG-related conditions.

Tongji-ECG Dataset The Tongji-ECG Dataset contains 270,112 ECGs with corresponding ICD-coded diagnostic information from 220,187 patients across three campuses of Tongji Hospital,

(a)



Large-scale, multicenter, multinational ECG: 13,348,593 ECGs, 2,984,209 patients

(b)

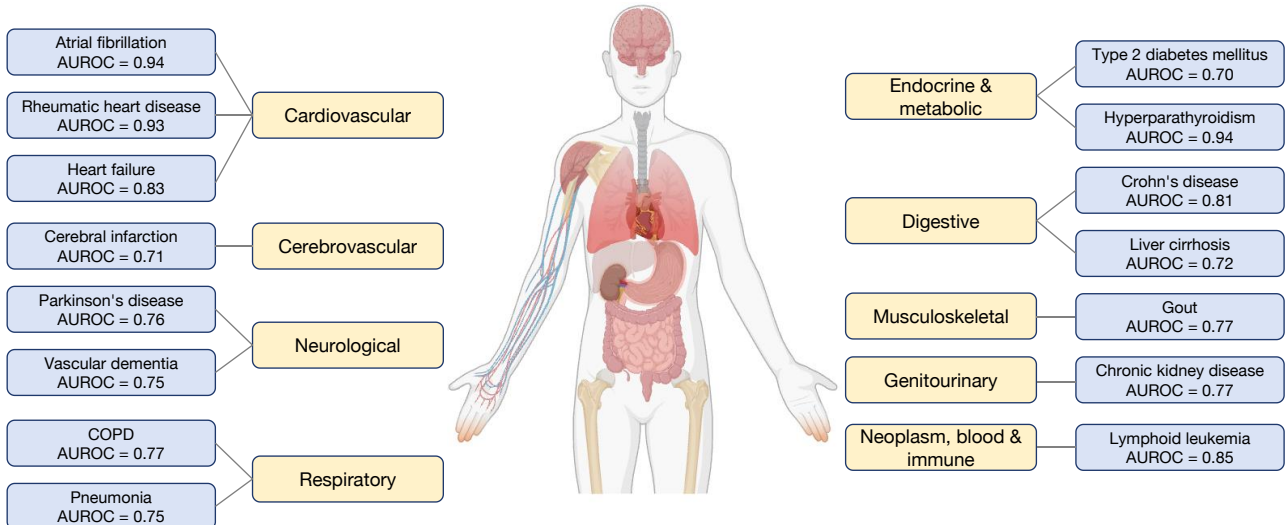


Figure 1: Overview of the development and results of AnyECG. (a) The source and composition of the dataset. The dataset we used included large-scale, multicenter, multinational ECG cohorts: 13,348,593 ECGs, 2,984,209 patients. (b) Representative results of AnyECG across different systems are presented. Outcome indicators for different diseases are shown across nine systems.

Huazhong University of Science and Technology (Main Campus, Optical Valley Campus, and Sino-French New City Campus) in Wuhan, China. Data were collected between 2017 and 2024, with patient demographic characteristics summarized in Supplementary. All 12-lead ECGs were sampled at 500 Hz, with a duration of 10 seconds.

PKUPH-ECG Dataset The PKUPH-ECG Dataset comprises 130,896 ECGs from 72,274 patients, each with ICD-coded diagnostic information. Data span from 2013 to 2024, with patient demographics summarized in Supplementary. All ECGs were recorded using a 12-lead configuration, sampled at 500 Hz, with a duration of 10 seconds.

CKB-ECG Dataset The CKB-ECG Dataset is a large population-based prospective cohort of more than 500,000 participants aged 30–79 years, recruited from ten geographically diverse regions across China²⁷. Among them, 44,336 participants underwent 12-lead ECG recording as part of extensive phenotyping, with data linked to detailed demographic, lifestyle, environmental, and clinical information, as well as genomic data from genome-wide genotyping and whole-genome sequencing in selected subsets.

MIMIC-ECG Dataset The MIMIC-ECG (MIMIC-IV-ECG) Dataset is a large-scale collection of 800,035 diagnostic 12-lead ECG recordings from 161,352 patients treated at Beth Israel Deaconess Medical Center (BIDMC) in Boston, USA³⁰. These ECGs are linked to the MIMIC-IV electronic health record, providing rich clinical context including diagnoses, medications and laboratory measurements. The diagnostic ECGs were acquired as part of routine care across the emergency department, intensive care units and outpatient facilities, and cover the period from 2008 to 2019. All waveforms are standard 10-second, 12-lead recordings sampled at 500 Hz, enabling direct comparison with other contemporary clinical ECG datasets.

PTB-XL Dataset The PTB-XL Dataset is a large, freely accessible clinical ECG corpus curated by the Physikalisch-Technische Bundesanstalt (PTB) in Germany²⁸. It comprises 21,837 10-second 12-lead ECG recordings from 18,885 patients, with extensive cardiologist-verified diagnostic labels organized in a hierarchical taxonomy. Recordings were collected at PTB between October 1989 and June 1996 as part of long-term ECG research and later converted into a standardized Dataset. Each ECG is available at the original sampling frequency of 500 Hz (with an additional downsampled 100 Hz version), making PTB-XL a widely used benchmark for supervised and self-supervised ECG modeling.

UKBB-ECG Dataset The UKBB-ECG Dataset is derived from the UK Biobank, a large prospective cohort of around 500,000 participants recruited across the United Kingdom³¹. Digital 12-lead ECGs were acquired at-rest imaging visits, yielding ECG measurements in 65,610 individuals from the general UK population. UK Biobank Resting ECGs were recorded at dedicated UK Biobank Imaging Assessment Centres using GE Cardiosoft systems, stored as XML files (Data-Field 20205). Each record is a 10-second, 12-lead tracing sampled at 500 Hz with 5,000 data points per lead, providing high-resolution waveforms suitable for large-scale genetic and phenotypic association studies.

CODE-15 ECG Dataset The CODE-15 ECG Dataset is a large, population-based Dataset constructed as a stratified 15% sample of the Brazilian CODE (Clinical Outcomes in Digital Electrocardiology) cohort²⁹. It contains 345,779 12-lead ECG examinations from 233,770 patients, collected by the Telehealth Network of Minas Gerais across 800+ municipalities in the state of Minas Gerais, Brazil. ECGs were acquired during routine telehealth care between 2010 and 2016, with recordings stored as digital waveforms and linked to clinical reports. Signals are standard 12-lead recordings sampled at 400 Hz, with variable duration (a large subset of 143,328 exams providing 10-second segments), making CODE-15 one of the largest publicly available ECG datasets for developing and benchmarking deep-learning models for automatic ECG diagnosis and risk prediction.

Data Preprocessing

The data preprocessing in this study followed a standardized and rigorous process. First, damaged, incomplete, or metadata-inconsistent records were removed. Then, all ECG signals with sampling frequencies below 500 Hz were resampled to 500 Hz using linear interpolation. Next, a 50/60 Hz notch filter was used to suppress power line interference, followed by a fourth-order Butterworth bandpass filter (0.67–40 Hz) to preserve physiologically relevant components while reducing high- and low-frequency noise. Finally, baseline drift was corrected by subtracting a 0.4-second median-filtered baseline estimate. This process ensured that the final signal retained the 0.67–40 Hz frequency band while minimizing noise, power line artifacts, and drift. For records longer than 10 seconds, consecutive 10-second segments were extracted; for shorter records, zero-padding was used. All signals were normalized using the mean and standard deviation of each segment before being input into the model.

Matching ECGs and ICDs

To achieve systematic prediction of multiple disease spectrums based on ECG, we matched discharge ICD diagnoses in patients' electronic health records (EHR) with their corresponding ECG one-to-one, and constructed a scalable data integration workflow to form a high-quality ECG-ICD diagnosis matching queue.

At the coding level, we first standardized all ICD diagnoses, including removing leading zeros and standardizing the coding format, to minimize biases caused by differences in recording methods across centers and time periods. The cleaned ICD codes were further converted into multi-label binary matrices, allowing for a structured representation of all diagnostic information for each patient, thus adapting to the multi-label output requirements of deep learning models. To enhance clinical interpretability, we mapped all ICD codes to standardized diagnostic names and systematically cleaned up redundant labels caused by differences in coding rules.

In the data alignment stage, we synchronized ECG records with patient discharge times, ensuring correct alignment by matching time intervals and patient identifiers. Only patients with valid ECG data at discharge were included in the final analysis queue. The process ensures the temporal correlation and clinical consistency between diagnostic labels and ECG signals, thereby significantly improving the reliability and clinical significance of downstream model training.

Finally, we systematically grouped all paired data according to the first letter of the ICD code (i.e., the top-level diagnostic system), allowing the predictive performance of different disease systems to be evaluated independently. Through this series of rigorous coding standardization, label construction, data alignment, and hierarchical processing, we built a high-quality, multi-disease, multi-label large-scale ECG-diagnostic cohort, providing a solid data foundation for subsequent model training, generalization evaluation, risk prediction, and comorbidity identification.

AnyECG Development

We construct an advanced deep learning architecture based on the Net1D framework and integrate an attention mechanism to enhance spatiotemporal feature extraction from ECG data³². This architecture adopts a hierarchical feature learning design: capturing low-level morphological features in the initial layer and progressively refining them into high-level spatiotemporal feature representations in deeper layers. To achieve this, we introduce a series of bottleneck modules that significantly enhance feature expressiveness while maintaining computational efficiency through collaborative grouped convolutions and channel attention mechanisms. Details of pre-training have been described in our previous work.

For downstream task adaptation, we employ a transfer learning strategy. We retain the pre-trained backbone network parameters and replace the original classification head with a task-specific linear projection layer, whose output neuron count is aligned with the category dimension of the target task. The model’s training objective is to achieve accurate classification output by minimizing the difference between the predicted distribution and the true label.

All algorithms studied are implemented using the PyTorch framework and trained on a GPU cluster consisting of 8 NVIDIA RTX 4090 GPUs. Model optimization employed the AdamW optimizer with an initial learning rate of 1×10^{-4} and weight decay of 1×10^{-5} . Training lasted for 30 epochs, during which the learning rate was dynamically adjusted using cosine annealing. The batch size per GPU was set to 256. To ensure the model’s generalization ability and effectively mitigate overfitting, an early stopping mechanism was implemented: training was automatically terminated if the validation set loss showed no improvement for 5 consecutive epochs.

Evaluation and Statistical Analysis

Model performance was comprehensively assessed using the Area Under the Receiver Operating Characteristic curve (AUROC) to evaluate global discriminative capacity.

To provide a granular evaluation, we further reported Sensitivity, Specificity, and the F1-score. Sensitivity quantified the model’s capacity to correctly identify positive cases:

$$\text{Sensitivity} = \frac{\text{TP}}{\text{TP} + \text{FN}} \quad (1)$$

Specificity measured the accuracy in excluding negative controls:

$$\text{Specificity} = \frac{\text{TN}}{\text{TN} + \text{FP}} \quad (2)$$

The F1-score, calculated as the harmonic mean of precision and recall, served as a robust metric for overall classification accuracy, particularly in the context of class imbalance:

$$F1 = 2 \cdot \frac{\text{Precision} \cdot \text{Recall}}{\text{Precision} + \text{Recall}} \quad (3)$$

Results

AnyECG Demonstrates Excellent Performance in Cardiovascular Disease Detection

Here, we report the internal and external validation performance of AnyECG across a spectrum of ECG-recognizable cardiovascular diseases. Internal validation was conducted using a patient-level split of the MGH-ECG cohort, whereas the Tongji-ECG dataset was used for external testing. AnyECG achieved robust and consistent discrimination across all classical ECG-detectable abnormalities. For atrial fibrillation and flutter, AUROC reached 0.949 (95% CI: 0.943–0.954) internally and 0.884 (95% CI: 0.881–0.887) externally. Paroxysmal tachycardia was similarly well identified (internal AUROC: 0.852 [95% CI: 0.839–0.868]; external AUROC: 0.841 [95% CI: 0.836–0.846]). Conduction disorders, including atrioventricular and left bundle-branch blocks, were also identified with excellent accuracy, achieving an internal AUROC of 0.912 (95% CI: 0.900–0.923) and an external AUROC of 0.847 (95% CI: 0.843–0.851). Acute myocardial infarction demonstrated outstanding internal discrimination with an AUROC of 0.954 (95% CI: 0.949–0.958), while maintaining strong generalizability externally with an AUROC of 0.850 (95%

CI: 0.845–0.858). Cardiomyopathy achieved the highest performance among all evaluated disease categories, with an internal AUROC of 0.957 (95% CI: 0.951–0.962) and an external AUROC of 0.866 (95% CI: 0.864–0.869).

Beyond these traditional targets, AnyECG achieved meaningful discrimination for structural and systemic cardiovascular diseases that traditionally lack definitive ECG signatures. For non-rheumatic mitral valve disease, performance reached an internal AUROC of 0.889 (95% CI: 0.883–0.895) and an external AUROC of 0.764 (95% CI: 0.759–0.774), whereas multi-valve involvement was identified with an internal AUROC of 0.932 (95% CI: 0.914–0.947) and a notably strong external AUROC of 0.926 (95% CI: 0.901–0.949). Non-rheumatic aortic valve disease yielded an internal AUROC of 0.915 (95% CI: 0.906–0.925) and an external AUROC of 0.893 (95% CI: 0.889–0.899), and rheumatic tricuspid valve disease achieved an internal AUROC of 0.918 (95% CI: 0.902–0.931) with an external AUROC of 0.810 (95% CI: 0.797–0.825).

AnyECG also demonstrated capability in detecting coronary syndromes beyond infarction: angina pectoris achieved an internal AUROC of 0.728 (95% CI: 0.723–0.732) and an external AUROC of 0.663 (95% CI: 0.659–0.666), while acute ischemic heart disease showed an internal AUROC of 0.814 (95% CI: 0.808–0.819) and a strong external AUROC of 0.932 (95% CI: 0.928–0.933). For heart failure, the model achieved an internal AUROC of 0.839 (95% CI: 0.835–0.842) and an external AUROC of 0.783 (95% CI: 0.780–0.785).

Hypertension and its sequelae were also identifiable: primary hypertension yielded AUROCs of 0.739 (95% CI: 0.735–0.742) internally and 0.753 (95% CI: 0.752–0.755) externally; hypertensive heart disease, 0.887 (95% CI: 0.878–0.896) internally and 0.788 (95% CI: 0.777–0.797) externally; and hypertensive chronic kidney disease, 0.759 (95% CI: 0.718–0.793) internally and 0.705 (95% CI: 0.701–0.711) externally. Finally, cerebral infarction was detected with internal validation of (AUROC: 0.717 [95% CI: 0.707–0.728]) and external validation of (AUROC: 0.701 [95% CI: 0.698–0.703]) for each respective condition.

Importantly, even for these non-classical ECG targets, internal AUROC values commonly remained in the mid-0.80s, with only modest performance attenuation (typically 0.10–0.15) in external cohorts, underscoring the broad phenotypic sensitivity and real-world generalizability of the model.

Overall, these results highlight AnyECG's dual strengths: high-level performance on established ECG interpretations and novel detection of structural, ischemic, hypertensive, and cerebrovascular pathologies, thereby extending the ECG's utility as a universal, noninvasive screening modality.

AnyECG Facilitates Comprehensive Disease Detection

Building on AnyECG's strong diagnostic capabilities for cardiovascular diseases, we next extended its scope to the detection of diseases across all major body systems. These include, but are not limited to, the nervous system, eye and ear disorders, the respiratory system, the genitourinary system, the digestive system, endocrine, nutritional, and metabolic diseases, neoplasms, blood and immune disorders, and the musculoskeletal system.

Figure 2 summarises performance across chapters. Median AUROC values ranged from 0.78 for psychology disease to 0.80 for circulatory diseases, with genitourinary (median 0.65) and respiratory (median 0.66) also exhibiting strong aggregate signals. In total 588 of the 1,172 phenotypes (50.2 %) achieved AUROC ≥ 0.65 (Bonferroni-corrected $p < 0.01$); 90 phenotypes surpassed an AUROC of 0.85 (Supplementary Table A).

Endocrine & metabolic – Disorders of mineral metabolism were predicted with exceptional accuracy (AUROC: 0.884 [95% CI: 0.882–0.885]), while common metabolic phenotypes such as type 2 diabetes mellitus still attained an AUROC of 0.703 (95% CI: 0.697–0.707).

Mental & behavioural – Vascular dementia (AUROC 0.757 [95% CI: 0.757-0.758]) and Parkinson’s disease (AUROC 0.761 [95% CI: 0.723-0.797]) showed a markedly high signal, echoing emerging evidence that autonomic and conduction abnormalities accompany neurodevelopmental disorders.

Neoplastic diseases – Among Lymphoid leukemia (AUROC: 0.855 [95% CI: 0.850-0.859]) and leukemia of unspecified cell type (AUROC: 0.798 [95% CI: 0.792-0.802]) were the most accurately anticipated.

Respiratory system – Chronic obstructive pulmonary disease, pneumonia and respiratory failure reached AUROC values of 0.773 [95% CI: 0.759-0.786], 0.750 [95% CI: 0.745-0.755] and 0.740 [95% CI: 0.730-0.750], respectively, indicating that subclinical gas-exchange or autonomic changes are already encoded in the ECG.

Digestive system – Crohn’s disease was predicted well (AUROC: 0.817 [95% CI: 0.774-0.857]), aligning with studies linking intestinal inflammation to cardiac electrophysiology via systemic cytokine release.

Genitourinary system – Kidney failure (AUROC: 0.821 [95% CI: 0.812-0.832]) and chronic kidney disease (AUROC: 0.765 [95% CI: 0.759-0.771]) both surpassed clinical utility thresholds.

All highlighted phenotypes retained statistical significance after multiplicity correction. Importantly, many of the strongest signals (e.g. cardiomyopathy, disorders of mineral metabolism, lymphoid leukemia) involve pathophysiological mechanisms—myocardial remodeling, hormonal milieu, autonomic dysregulation—that plausibly manifest as subtle but learnable ECG patterns years before clinical recognition.

These results extend the utility of the resting ECG well beyond cardiovascular medicine, demonstrating that a foundation ECG model captures latent signatures of endocrine, oncological, respiratory and neuropsychiatric pathology. By illuminating hundreds of pre-symptomatic risk markers across diverse organ systems, our work positions the ECG as a scalable, low-cost screening modality for population-level precision health initiatives.

AnyECG Demonstrates Potential for Future Disease Prediction

We next asked whether a single 12-lead tracing could yield actionable prognostic information across the cardio-kidney-metabolic (CKM) spectrum. We evaluated AnyECG leveraging 44,336 ECGs from the CKB. For each of the eight most prevalent CKM conditions we allocated participants to low-, medium-, or high-risk tertiles and evaluated incident disease-free survival over a median follow-up of 8 years.

In all CKM-related diseases evaluated, AnyECG demonstrated clear and statistically significant separation of Kaplan-Meier survival curves (log-rank $p < 0.001$ for all comparisons; Figures 4a-d and 5a-d). For example, in essential hypertension (Fig. 4a), consistent with clinical expectations, the 10-year disease-free survival rate was markedly lower in the high-risk group than in the low-risk group (83.7% vs. 94.4%), with a hazard ratio (HR) of 2.08 (95% CI 1.95–2.22). Acute myocardial infarction (Fig. 4b) exhibited a similarly pronounced difference (97.2% vs. 99.4%; HR = 2.41, 95% CI 2.15–2.70). Atrial fibrillation (Fig. 4c) showed a 10-year survival of 92.0% versus 98.0% between the high- and low-risk groups (HR = 2.46, 95% CI 2.28–2.65), and heart failure (Fig. 4d) displayed a comparable separation (95.6% vs. 99.0%; HR = 2.73, 95% CI 2.43–3.07).

Systemic CKM diseases demonstrated similarly robust risk stratification. Cerebral infarction (Fig. 5a) showed survival rates of 97.8% versus 99.5% (HR = 2.18, 95% CI 1.96–2.42), type 2 diabetes mellitus (Fig. 5b) 95.1% versus 98.6% (HR = 2.29, 95% CI 2.12–2.47), chronic kidney disease (Fig. 5c) 96.3% versus 98.9% (HR = 2.11, 95% CI 1.96–2.27), and gout (Fig. 5d) 96.9% versus 99.1% (HR = 2.05, 95% CI 1.88–2.24).

Together, these results highlight that a single resting ECG, interpreted by AnyECG, captures

latent systemic health signals associated with CKM disease development, enabling clinically actionable and scalable population-level risk stratification.

Even for diseases with extremely low absolute incidence, such as acute myocardial infarction and cerebral infarction, AnyECG still produced narrow confidence intervals and significant discrimination, highlighting the statistical robustness and practical predictive power of the model-derived biomarkers. In summary, a single resting electrocardiogram interpreted by AnyECG can capture the implicit characteristics of systemic health status, and its applicability extends beyond the traditional risk prediction paradigm centered on cardiac endpoints. This method provides a simultaneously available, multi-indicator consistent risk assessment capability for common chronic diseases, laying an important foundation for low-cost, non-invasive, scalable population risk stratification and precision prevention strategies.

AnyECG Reveals Links Between Comorbidities

We quantified pair-wise associations between all model-derived risk scores in the 220,187 Tongji-ECG participants and visualised the results with complementary network, scatter-plot and heat-map representations (Fig. 6).

The rank-correlation heat-map of all diseases (Fig. 6a) displayed a striking block-diagonal architecture. A highly cohesive cardiometabolic module—comprising essential hypertension (HPT), atrial fibrillation (AF), myocardial infarction (I21), cerebral infarction (I64) and rheumatic heart disease (RHD)—showed a median Spearman $r = 0.42$ (inter-quartile range, IQR 0.38–0.48). Pulmonary (COPD), kidney (CKD) and metabolic (type 2 diabetes mellitus, T2DM; gout) conditions clustered separately (median intra-cluster $r = 0.28$), whereas neuro-degenerative and anaemia-related codes (Parkinson’s disease, PD; vascular dementia, VaD; iron-deficiency anaemia, IDA) formed a comparatively weakly connected community (median $r = 0.07$). These patterns mirror epidemiological studies, suggesting that AnyECG eyes the same latent pathophysiology directly from electrical activity.

The chord diagram for the 15 most common conditions (Fig. 6b) translated the correlation matrix into an interpretable network: link width encodes mutual information and colour denotes direction (red positive, blue negative). Hypertension emerged as the most central node (weighted degree = 33.7), radiating strong connections to AF, T2DM and CKD, followed by AF (degree = 31.2) and CKD (degree = 29.5). Disease-specific subnetworks underscore clinically recognised cascades:

Individual-level scatter plots confirm selective, not global, correlations. To exclude the possibility that AnyECG simply assigns uniformly high risk to sicker individuals, we inspected representative bivariate distributions. Predicted stroke (I64) and myocardial infarction (I21) scores were tightly co-distributed (Spearman $r = 0.67$; Fig. 6g), whereas Parkinson’s disease (G30) and stroke scores were almost uncorrelated ($r = 0.05$; Fig. 6h). Similarly, kidney disease (N18) and ischaemic bowel disease (I25) predictions showed no appreciable structure ($r = 0.02$; Fig. 6i). Thus, the comorbidity signal is specific, not an artefact of a generic “bad ECG” phenotype.

These analyses demonstrate that AnyECG does not treat diseases as isolated endpoints; instead, it learns a latent representation that encodes the complex topology of human multimorbidity. By jointly modelling cross-organ interactions, an inexpensive resting ECG can therefore serve as a non-invasive window into an individual’s integrated disease trajectory—a capability with immediate relevance for differential diagnosis, risk-aligned screening programmes, and cluster-targeted precision prevention.

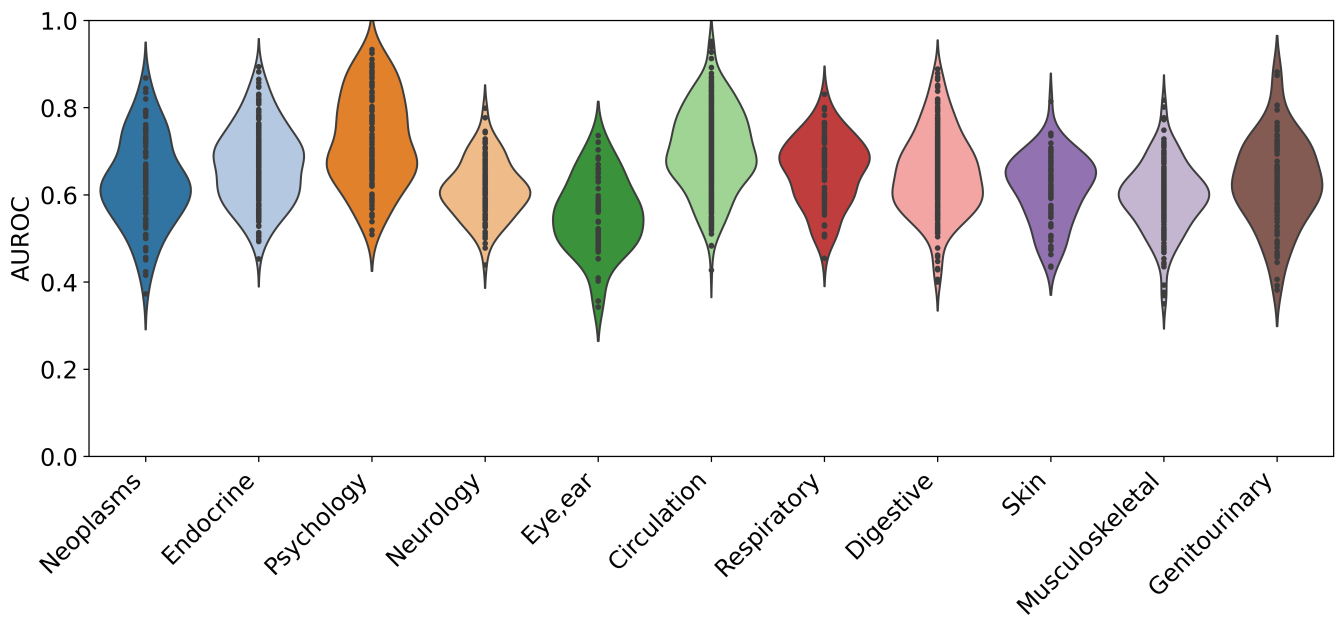


Figure 2: Boxplots for the overall internal test set performance of AnyECG on different disease systems.

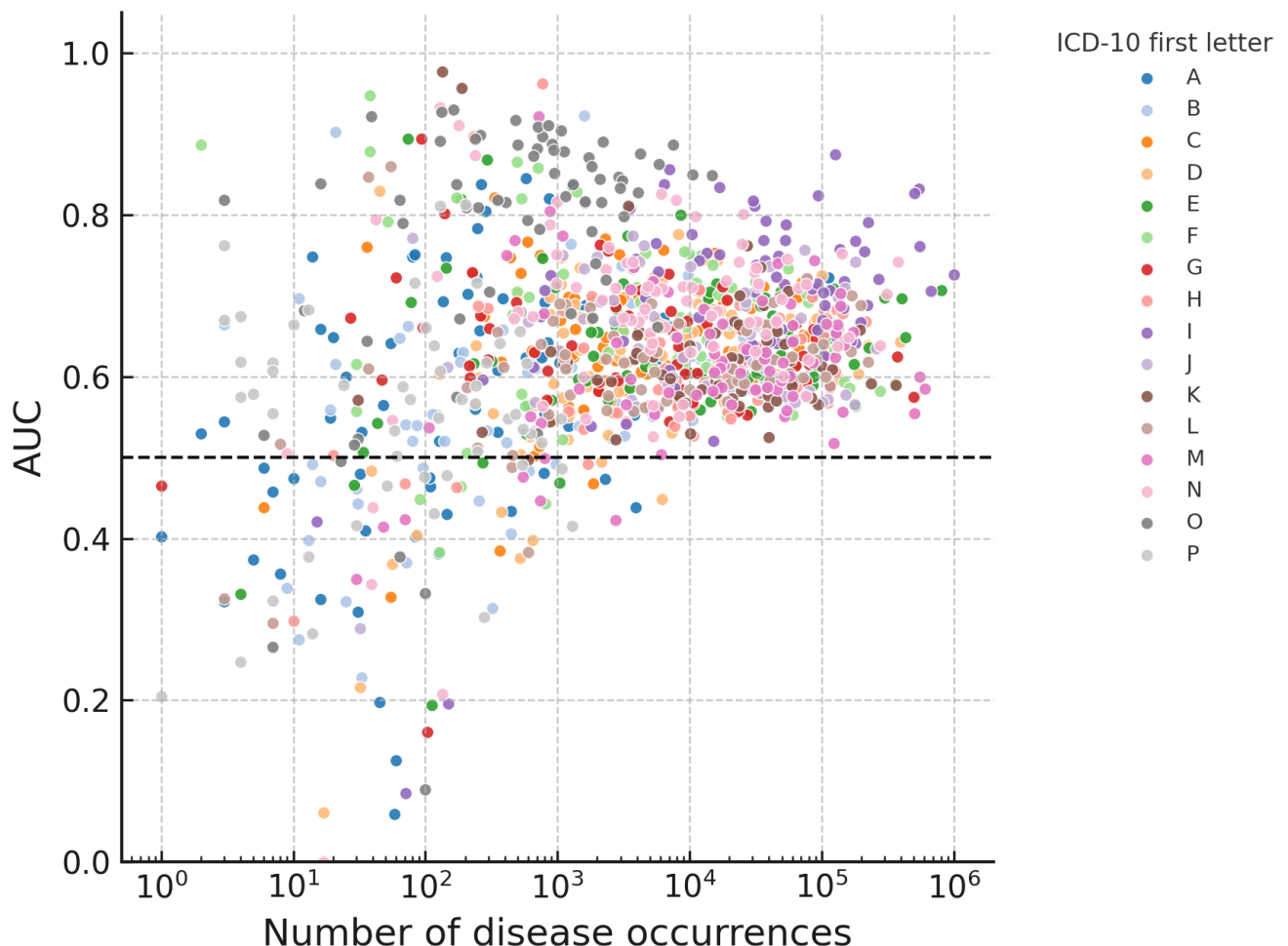
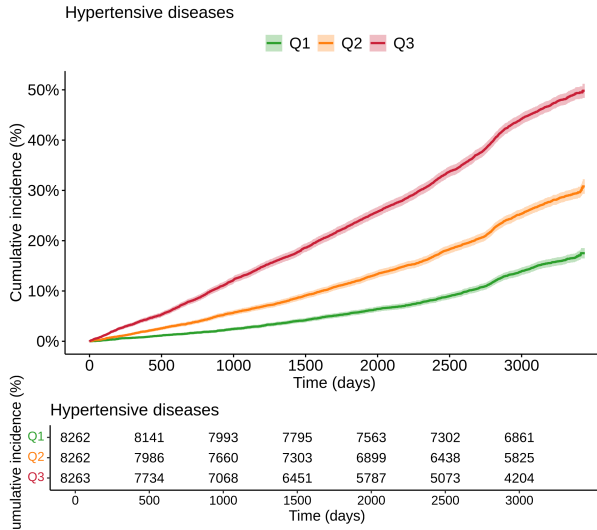
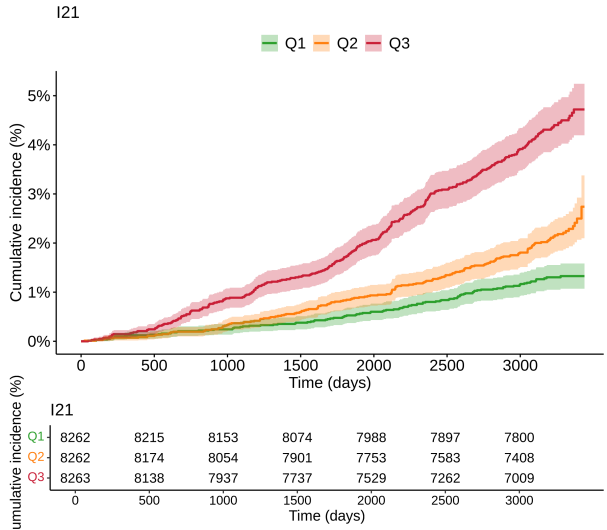


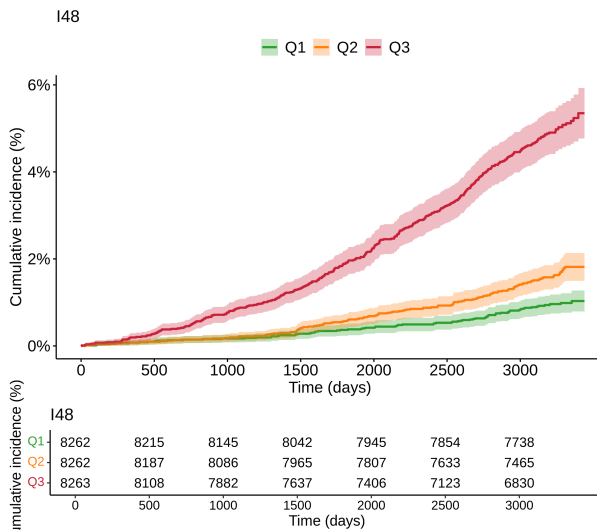
Figure 3: Average diagnosis AUC values (y axis) as a function of training occurrences (x axis).



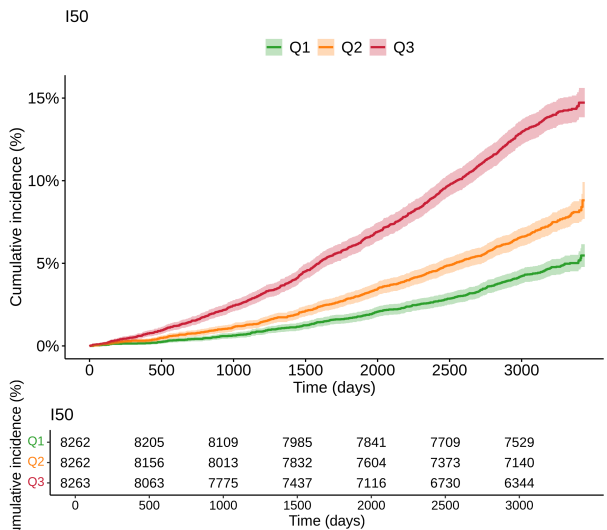
(a) Hypertensive diseases



(b) Acute myocardial infarction



(c) Atrial fibrillation and flutter



(d) Heart failure

Figure 4: Prognostic stratification of major cardiometabolic cardiac events using AnyECG in the CKB cohort.

Discussion

In our study, we have developed a comprehensive hybrid model for diagnosing various diseases across different human systems, using the electrocardiogram (ECG) as the sole input. Utilizing the Tongji-ECG dataset as the training set and a large Dataset from prominent tertiary hospitals in China as an external validation set, we have doubly confirmed the potential of ECG in diagnosing a broad spectrum of diseases. This provides a scientific basis for future single-modal, non-invasive, and early full-spectrum diagnoses using ECG alone.

Revolutionizing ECG as a Systemic Diagnostic Tool

The AnyECG model represents a paradigm shift in electrocardiography, demonstrating unprecedented capacity to detect latent cardiovascular disease (CVD) and diverse non-cardiac conditions years before clinical manifestation. Specifically, ECG as a standard way in recording the electrical

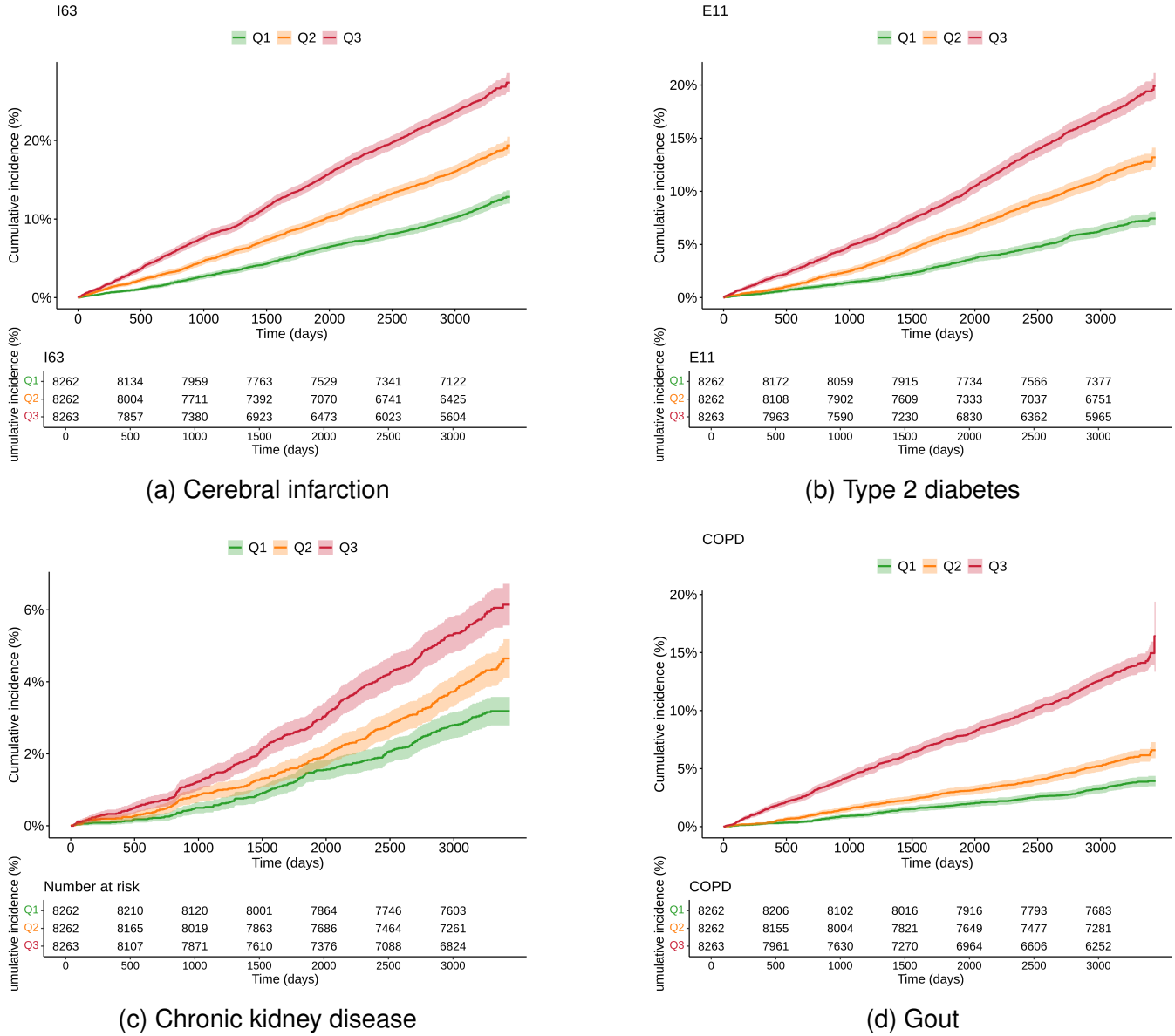


Figure 5: Prognostic stratification of systemic CKM diseases using AnyECG in the CKB cohort.

activity of heart, shows specific performance in detecting abnormalities in cardiovascular diseases. In our study, its exceptional performance for cardiomyopathy (AUROC 0.95), AMI (AUROC 0.95), structural heart diseases (AUROC 0.94), and atrial fibrillation (AUROC 0.94) aligns with known electrophysiological substrates but extends beyond current clinical expectations, indicating the consistent and excellent monitoring performance of AI-enabled model in a wide spectrum of cardiovascular disease system. More remarkably, the model identified high-risk signatures for conditions spanning endocrine (puberty disorders, AUROC 0.98), neuropsychiatric (ADHD, AUROC 0.99), oncologic (breast cancer, AUROC 0.83), and gastrointestinal diseases (Crohn's, AUROC 0.82). This evidences that ECG morphology encodes systemic pathophysiology—likely mediated through autonomic nervous system dysregulation, inflammatory cascades, or metabolic stress—transforming the ECG from a cardiac-specific tool into a holistic biomarker platform. For example, Sunil Vasu Kalmady developed a machine learning algorithms based on electrocardiograms for cardiovascular diagnoses at the population level.³³ Nils Strodthoff et.al. construct an explorative study in emergency care using AI-enhanced ECG as a screening tool for cardiac

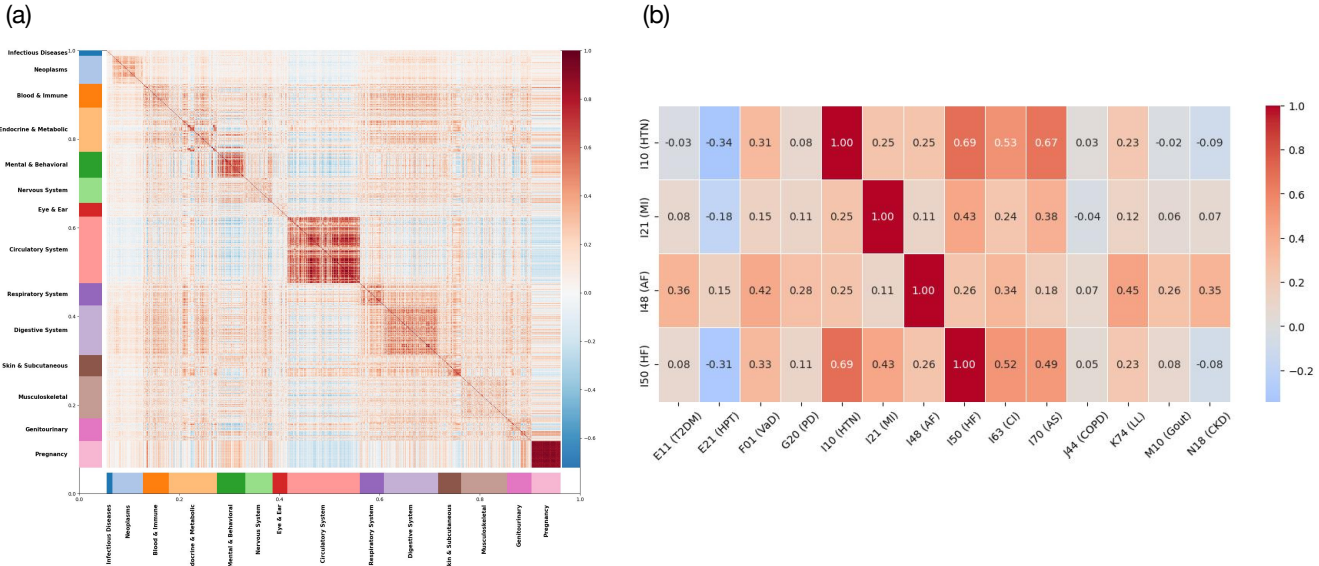


Figure 6: Model-derived disease co-occurrence patterns and correlation structure. (A) Chord diagram showing pairwise associations between selected chronic diseases, where ribbon width reflects the strength of association and ribbon color encodes the sign and magnitude (red: stronger positive association; blue: negative/weaker association). Disease segments on the circumference are colored by clinical system (e.g., cardiovascular, metabolic, kidney, respiratory). (B) Correlation heatmap between columns of the model output, illustrating the global correlation structure across all predicted disease labels and revealing blocks of tightly correlated conditions along the diagonal.

and non-cardiac conditions.³⁴ Sam F. Friedman analyzed ECG encodings and different diseases Phecodes using AI model and found that the strongest ECG association was with hypertension.³⁵ Building on the aforementioned studies, our research has taken a further step by conducting a more comprehensive and broad-spectrum analysis of the end-to-end diagnostic links between ECG and individual diagnoses across various systems.

ECG as Novel Digital Biomarkers for Systemic Diseases to Explore the Mechanistic Plausibility and Biological Insights

The observed discriminative power finds strong biological grounding in shared subclinical pathways. Conditions with peak accuracy—cardiomyopathy, ADHD, and puberty disorders involve autonomic remodeling or hormonal modulation known to alter repolarization dynamics and conduction stability.³⁶ Core symptoms of ADHD (such as attention deficit and hyperactivity) are closely associated with autonomic nervous dysfunction (e.g., sympathetic hyperactivity), suggesting that similar mechanisms may underlie the link between neurodevelopmental disorders and electrophysiological abnormalities.³⁷ Hormonal dysregulation (e.g., thyroid hormones and sex hormones) can directly influence repolarization dynamics and conduction stability by altering the expression of myocardial ion channels.^{38,39} Patients with puberty disorders often exhibit hormonal fluctuations, which may induce electrophysiological remodeling analogous to paraneoplastic arrhythmias, manifesting as QT interval prolongation or premature ventricular contractions.⁴⁰ Similarly, inflammatory states (e.g., Crohn's disease) may drive electrophysiological shifts via cytokine-mediated ion channel dysfunction,^{41,42} while metabolic disorders like obesity (AUROC 0.90) likely manifest through myocardial substrate utilization defects. For oncology, the prediction of breast and thyroid cancers years before diagnosis supports emerging literature on paraneoplastic electrophysiological remodeling.^{43,44} Ben G T Coumbe et.al. reports electrophysiological

abnormalities resulting from autonomic nervous dysfunction in patients with breast cancer and other malignancies, and cardiac autonomic nervous dysfunction in cancer patients encompasses electrophysiological abnormalities such as paraneoplastic arrhythmias.⁴⁵ These findings suggest ECG signatures reflect not only structural cardiac changes but also neuroendocrine, inflammatory, and metabolic cross-talk, enabling early risk stratification across organ systems.

Endow ECG with New Applications in Detecting Comorbidities and Predicting Future Diseases

In our study, we found that there are close associations between different system diseases, as well as in different diseases in one system, indicating the ECG foundation model has endowed ECG new applications for diagnosing comorbid diseases. For example, Hypertension is one of the most common and potent risk factors for developing atrial fibrillation.⁴⁶ While chronically high blood pressure forces the heart to work harder causing Left Ventricular Hypertrophy (LVH), left Atrial Enlargement, fibrosis and Electrical Remodeling, which serves as the reason of AF.⁴⁷ Besides, HTN often coexists with other AF risk factors including coronary artery disease (CAD) and heart failure (HF), which strengthen the association of AF and HTN.⁴⁸ Further, Uncontrolled hypertension damages the delicate blood vessels (glomeruli) in the kidneys over time, reducing their filtering ability.⁴⁹ At the meantime, CKD induced deficient ability to regulate fluid and electrolyte balance, and thus activate the Renin-Angiotensin-Aldosterone System (RAAS), and impair blood vessel function, which leads to progressive HTN.⁵⁰

Further, we found potential interactions between COPD and RHD, where there seems no direct causal link like the previous pairs. The interaction mechanism may origins from Pulmonary Hypertension (PH). Severe COPD can lead to PH, and increase the pressure in the right side of the heart.⁵¹ If RHD has caused right-sided valve disease (like tricuspid stenosis/regurgitation), this pre-existing damage is significantly worsened by the increased workload from PH.⁵² Besides, hypoxia and Inflammation in COPD can exacerbate underlying heart disease including RHD.^{53,54} Thus the ECG-foundation model not only shows consisted mechanisms, but also exhibits potential and latent mechanism compared to the previous studies. This indicates it a valuable tool in diseases treatment and prognosis prediction.

Conclusion

In conclusion, this study fundamentally transforms the diagnostic potential of the electrocardiogram (ECG). Through the development and rigorous external validation of the AnyECG model, we demonstrate that AI-powered analysis of a single, standard ECG can provide highly accurate diagnosis (as evidenced by high AUROCs) not only for a wide spectrum of cardiovascular diseases (e.g., cardiomyopathy, AMI, AF) but also for diverse non-cardiac conditions across endocrine, neuropsychiatric, oncologic, and gastrointestinal systems. This unprecedented systemic diagnostic capability is mechanistically plausible, grounded in ECG morphology capturing systemic pathophysiology mediated by autonomic nervous system dysregulation, hormonal modulation, inflammatory cascades, metabolic stress, and paraneoplastic effects and so on. Furthermore, the ECG foundation model reveals intricate associations and potential pathways linking comorbid diseases (e.g., HTN/AF, HTN/CKD, COPD/RHD via PH), offering valuable insights for early risk stratification, diagnosing complex comorbidities, and predicting long-term prognosis. Collectively, this research establishes the ECG as a powerful, non-invasive platform for holistic, early, and broad-spectrum disease detection across multiple organ systems.

ACKNOWLEDGMENTS

This work is supported by the National Natural Science Foundation of China (62102008, 62172018), CCF-Tencent Rhino-Bird Open Research Fund (CCF-Tencent RAGR20250108), CCF-Zhipu Large Model Innovation Fund (CCF-Zhipu202414), PKU-OPPO Fund (BO202301, BO202503), Research Project of Peking University in the State Key Laboratory of Vascular Homeostasis and Remodeling (2025-SKLVHR-YCTS-02). Hongling Zhu is funded by the National Key R&D Program of China (No. 2022YFE0209900), the National Natural Science Foundation of China (No. 82100531), Medical Artificial Intelligence Fund of Tongji Hospital (No. AI2024A02), Tongji Hospital Excellent Young Scientist Fund (No. 24-2KYC13057-14), Huazhong University of Science and Technology's 2024 "Interdisciplinary Research Support Program" Project (No. 2024JCYJ066-PP, 5003540166) and Tongji Hospital Medical Innovation and Translational Incubation Project (No. 2023CXZH004) .

References

1. Stracina, T., Ronzhina, M., Redina, R., and Novakova, M. (2022). Golden standard or obsolete method? review of ecg applications in clinical and experimental context. *Frontiers in Physiology* *13*, 867033.
2. Liu, X., Wang, H., Li, Z., and Qin, L. (2021). Deep learning in ecg diagnosis: A review. *Knowledge-Based Systems* *227*, 107187.
3. Lippi, G., Sanchis-Gomar, F., and Cervellin, G. (2021). Global epidemiology of atrial fibrillation: an increasing epidemic and public health challenge. *International journal of stroke* *16*, 217–221.
4. Wang, C.L., Wei, C.C., Tsai, C.T., Lee, Y.H., Liu, L.Y.M., Chen, K.Y., Lin, Y.J., and Lin, P.L. (2023). Early detection of myocardial ischemia in resting ecg: analysis by hht. *BioMedical Engineering OnLine* *22*, 23.
5. Kim, D.Y., Lee, S.W., Lee, D.H., Lee, S.C., Jang, J.H., Shin, S.H., Kim, D.H., Choi, W., and Baek, Y.S. (2025). Electrocardiography-based artificial intelligence predicts the upcoming future of heart failure with mildly reduced ejection fraction. *Frontiers in Cardiovascular Medicine* *12*, 1418914.
6. Attia, Z.I., and Friedman, P.A. (2023). Explainable ai for ecg-based prediction of cardiac resynchronization therapy outcomes: learning from machine learning?. Oxford University Press US.
7. Turgut, Ö., Müller, P., Hager, P., Shit, S., Starck, S., Menten, M.J., Martens, E., and Rueckert, D. (2025). Unlocking the diagnostic potential of electrocardiograms through information transfer from cardiac magnetic resonance imaging. *Medical Image Analysis* *101*, 103451.
8. Deng, C., Niu, J., Xuan, L., Zhu, W., Dai, H., Zhao, Z., Li, M., Lu, J., Xu, Y., Chen, Y. et al. (2020). Association of qtc interval with risk of cardiovascular diseases and related vascular traits: a prospective and longitudinal analysis. *Global heart* *15*, 13.
9. Buszman, P., Szafranek, A., Kalarus, Z., and Gasior, M. (1995). Use of changes in st segment elevation for prediction of infarct artery recanalization in acute myocardial infarction. *European heart journal* *16*, 1207–1214.
10. Chen, S.W., Wang, S.L., Qi, X.Z., Samuri, S.M., and Yang, C. (2022). Review of ecg detection and classification based on deep learning: Coherent taxonomy, motivation, open challenges and recommendations. *Biomedical Signal Processing and Control* *74*, 103493.
11. Attia, I.Z., Tseng, A.S., Benavente, E.D., Medina-Inojosa, J.R., Clark, T.G., Malyutina, S., Kapa, S., Schirmer, H., Kudryavtsev, A.V., Noseworthy, P.A. et al. (2021). External validation of a deep learning electrocardiogram algorithm to detect ventricular dysfunction. *International journal of cardiology* *329*, 130–135.
12. Dhingra, L.S., Aminorroaya, A., Pedroso, A.F., Khunte, A., Sangha, V., McIntyre, D., Chow, C.K., Asselbergs, F.W., Brant, L.C., Barreto, S.M. et al. (2025). Artificial intelligence–enabled prediction of heart failure risk from single-lead electrocardiograms. *JAMA cardiology* *10*, 574–584.

13. Holmstrom, L., Christensen, M., Yuan, N., Weston Hughes, J., Theurer, J., Jujavarapu, M., Fatehi, P., Kwan, A., Sandhu, R.K., Ebinger, J. et al. (2023). Deep learning-based electrocardiographic screening for chronic kidney disease. *Communications Medicine* 3, 73.
14. Kim, J., Yang, H.L., Kim, S.H., Kim, S., Lee, J., Ryu, J., Kim, K., Kim, Z., Ahn, G., Kwon, D. et al. (2024). Deep learning-based long-term risk evaluation of incident type 2 diabetes using electrocardiogram in a non-diabetic population: a retrospective, multicentre study. *Eclinicalmedicine* 68.
15. Chung, C.T., Lee, S., King, E., Liu, T., Armoundas, A.A., Bazoukis, G., and Tse, G. (2022). Clinical significance, challenges and limitations in using artificial intelligence for electrocardiography-based diagnosis. *International journal of arrhythmia* 23, 24.
16. Sontis, K.C., Noseworthy, P.A., Attia, Z.I., and Friedman, P.A. (2021). Artificial intelligence-enhanced electrocardiography in cardiovascular disease management. *Nature Reviews Cardiology* 18, 465–478.
17. Moreno-Sánchez, P.A., García-Isla, G., Corino, V.D., Vehkaoja, A., Brukamp, K., Van Gils, M., and Mainardi, L. (2024). Ecg-based data-driven solutions for diagnosis and prognosis of cardiovascular diseases: A systematic review. *Computers in Biology and Medicine* 172, 108235.
18. Moosavi, A., Huang, S., Vahabi, M., Motamedivafa, B., Tian, N., Mahmood, R., Liu, P., and Sun, C.L. (2024). Prospective human validation of artificial intelligence interventions in cardiology: a scoping review. *JACC: Advances* 3, 101202.
19. Karabayir, I., and Akbilgic, O. (2025). Generalizability of electrocardiographic artificial intelligence. *npj Cardiovascular Health* 2, 38.
20. Muzammil, M.A., Javid, S., Afridi, A.K., Siddineni, R., Shahabi, M., Haseeb, M., Fariha, F., Kumar, S., Zaveri, S., and Nashwan, A.J. (2024). Artificial intelligence-enhanced electrocardiography for accurate diagnosis and management of cardiovascular diseases. *Journal of electrocardiology* 83, 30–40.
21. Moor, M., Banerjee, O., Abad, Z.S.H., Krumholz, H.M., Leskovec, J., Topol, E.J., and Rajpurkar, P. (2023). Foundation models for generalist medical artificial intelligence. *Nature* 616, 259–265.
22. Liu, X., Zhang, Y., Lu, Y., Yin, C., Hu, X., Liu, X., Chen, L., Wang, S., Rodriguez, A., Yao, H. et al. (2025). Biomedical foundation model: A survey. *arXiv preprint arXiv:2503.02104*.
23. McKeen, K., Masood, S., Toma, A., Rubin, B., and Wang, B. (2024). Ecg-fm: An open electrocardiogram foundation model. *arXiv preprint arXiv:2408.05178*.
24. Song, J., Jang, J.H., Lee, B.T., Hong, D., Kwon, J.m., and Jo, Y.Y. (2024). Foundation models for ecg: Leveraging hybrid self-supervised learning for advanced cardiac diagnostics. *arXiv preprint arXiv:2407.07110*.
25. Li, J., Aguirre, A.D., Junior, V.M., Jin, J., Liu, C., Zhong, L., Sun, C., Clifford, G., Brandon Westover, M., and Hong, S. (2025). An electrocardiogram foundation model built on over 10 million recordings. *NEJM AI* 2, Aloa2401033.
26. Koscova, Z., Li, Q., Robichaux, C., Moura Junior, V., Ghanta, M., Gupta, A., Rosand, J., Aguirre, A., Hong, S., Albert, D.E. et al. (2024). The harvard-emory ecg database. *medRxiv* pp. 2024–09.

27. Chen, Z., Chen, J., Collins, R., Guo, Y., Peto, R., Wu, F., and Li, L. (2011). China kadoorie biobank of 0.5 million people: survey methods, baseline characteristics and long-term follow-up. *International journal of epidemiology* *40*, 1652–1666.
28. Wagner, P., Strodtthoff, N., Bousseljot, R.D., Kreiseler, D., Lunze, F.I., Samek, W., and Schaeffter, T. (2020). Ptb-xl, a large publicly available electrocardiography dataset. *Scientific data* *7*, 1–15.
29. Ribeiro, A.H., Paixao, G., Lima, E.M., Ribeiro, M.H., Pinto Filho, M.M., Gomes, P.R., Oliveira, D.M., Meira Jr, W., Schon, T.B., and Ribeiro, A.L.P. (2021). Code-15%: A large scale annotated dataset of 12-lead ecgs. *Zenodo*, Jun 9, 10–5281.
30. Gow, B., Pollard, T., Nathanson, L.A., Johnson, A., Moody, B., Fernandes, C., Greenbaum, N., Berkowitz, S., Moukheiber, D., Eslami, P. et al. (2023). Mimic-iv-ecg-diagnostic electrocardiogram matched subset. Type: dataset.
31. Allen, N.E., Sudlow, C., Peakman, T., Collins, R., and biobank, U. (2014). Uk biobank data: come and get it. American Association for the Advancement of Science.
32. Hong, S., Xu, Y., Khare, A., Priambada, S., Maher, K., Aljiffry, A., Sun, J., and Tumanov, A. (2020). Holmes: Health online model ensemble serving for deep learning models in intensive care units. In *Proceedings of the 26th ACM SIGKDD International Conference on Knowledge Discovery & Data Mining*. pp. 1614–1624.
33. Kalmady, S.V., Salimi, A., Sun, W., Sepehrvand, N., Nademi, Y., Bainey, K., Ezekowitz, J., Hindle, A., McAlister, F., Greiner, R. et al. (2024). Development and validation of machine learning algorithms based on electrocardiograms for cardiovascular diagnoses at the population level. *npj Digital Medicine* *7*, 133.
34. Strodtthoff, N., Lopez Alcaraz, J.M., and Haverkamp, W. (2024). Prospects for artificial intelligence-enhanced electrocardiogram as a unified screening tool for cardiac and non-cardiac conditions: an explorative study in emergency care. *European Heart Journal-Digital Health* *5*, 454–460.
35. Friedman, S.F., Khurshid, S., Venn, R.A., Wang, X., Diamant, N., Di Achille, P., Weng, L.C., Choi, S.H., Reeder, C., Pirruccello, J.P. et al. (2025). Unsupervised deep learning of electrocardiograms enables scalable human disease profiling. *npj Digital Medicine* *8*, 23.
36. Sekaninova, N., Bona Olexova, L., Visnovcova, Z., Ondrejka, I., and Tonhajzerova, I. (2020). Role of neuroendocrine, immune, and autonomic nervous system in anorexia nervosa-linked cardiovascular diseases. *International Journal of Molecular Sciences* *21*, 7302.
37. Devine, M.F., Kothapalli, N., Elkhooly, M., and Dubey, D. (2021). Paraneoplastic neurological syndromes: clinical presentations and management. *Therapeutic Advances in Neurological Disorders* *14*, 1756286420985323.
38. Amin, A.S., Tan, H.L., and Wilde, A.A. (2010). Cardiac ion channels in health and disease. *Heart rhythm* *7*, 117–126.
39. Cao, Z., Zhou, Q., An, J., Guo, X., Jia, X., and Qiu, Y. (2025). Glycolytic dysfunction in granulosa cells and its contribution to metabolic dysfunction in polycystic ovary syndrome. *Drug Design, Development and Therapy* pp. 5255–5270.

40. D'Ascenzi, F., Solari, M., Anselmi, F., Valentini, F., Barbati, R., Palmitesta, P., Focardi, M., Bonifazi, M., and Mondillo, S. (2017). Electrocardiographic changes induced by endurance training and pubertal development in male children. *The American journal of cardiology* 119, 795–801.

41. Stringer, R.N., and Weiss, N. (2023). Pathophysiology of ion channels in amyotrophic lateral sclerosis. *Molecular Brain* 16, 82.

42. Werlein, C., Ackermann, M., Stark, H., Shah, H.R., Tzankov, A., Haslbauer, J.D., von Stillfried, S., Bülow, R.D., El-Armouche, A., Kuenzel, S. et al. (2023). Inflammation and vascular remodeling in covid-19 hearts. *Angiogenesis* 26, 233–248.

43. Iorio, R., Spagni, G., and Masi, G. (2019). Paraneoplastic neurological syndromes. In *Seminars in diagnostic pathology* vol. 36. Elsevier pp. 279–292.

44. Soomro, Z., Youssef, M., Yust-Katz, S., Jalali, A., Patel, A.J., and Mandel, J. (2020). Paraneoplastic syndromes in small cell lung cancer. *Journal of Thoracic Disease* 12, 6253.

45. Coumbe, B.G., and Groarke, J.D. (2018). Cardiovascular autonomic dysfunction in patients with cancer. *Current Cardiology Reports* 20, 69.

46. Kamioka, M., Narita, K., Watanabe, T., Watanabe, H., Makimoto, H., Okuyama, T., Yokota, A., Komori, T., Kabutoya, T., Imai, Y. et al. (2024). Hypertension and atrial fibrillation: the clinical impact of hypertension on perioperative outcomes of atrial fibrillation ablation and its optimal control for the prevention of recurrence. *Hypertension Research* 47, 2800–2810.

47. Rohla, M., and Rexhaj, E. (2025). Summary of the 2024 esc-guidelines for the management of elevated blood pressure and hypertension. *Praxis* 114, 48–50.

48. Potpara, T., Romiti, G.F., and Sohns, C. (2024). The 2024 european society of cardiology guidelines for diagnosis and management of atrial fibrillation: a viewpoint from a practicing clinician's perspective. *Thrombosis and haemostasis* 124, 1087–1094.

49. Suarez, M.L.G., Arriola-Montenegro, J., and Rolón, L. (2025). Hypertension management in patients with advanced chronic kidney disease with and without dialysis. *Current Opinion in Cardiology* 40, 199–205.

50. Halimi, J.M., Sarafidis, P., Azizi, M., Bilo, G., Burkard, T., Bursztyn, M., Camafort, M., Chapman, N., Cottone, S., de Backer, T. et al. (2024). Management of patients with hypertension and chronic kidney disease referred to hypertension excellence centres among 27 countries. on behalf of the european society of hypertension working group on hypertension and the kidney. *Blood pressure* 33, 2368800.

51. Mullen, E., McCullagh, B., Gaine, S., and Quadery, S.R. (2025). Recent advances in the diagnosis and management of pulmonary arterial hypertension. *British Journal of Hospital Medicine* 86, 1–13.

52. Rwebembera, J., and Beaton, A. (2024). Acute rheumatic fever and rheumatic heart disease: updates in diagnosis and treatment. *Current opinion in pediatrics* 36, 496–502.

53. Leitner, M., Blum, A.M., and Bals, R. (2025). Update copd and cardiovascular events. *Deutsche medizinische Wochenschrift (1946)* 150, 298–302.

54. Stieglitz, S., and Frohnhofer, H. (2025). Copd in elderly patients. *Pneumologie (Stuttgart, Germany)* 79, 382–394.

A Diagnostic performance of AnyECG for ICD-10 diagnoses

The diagnostic performance of AnyECG for ICD-10 codes with an AUC of at least 0.65 is summarized in Table A1, which covers ICD chapters I to XV and includes a total of 588 three-digit ICD-10 codes.

Table A1: Summary of ICD-10 codes with an AUC greater than 0.65 for AnyECG. ICD, International Classification of Diseases; AUC, area under the receiver operating characteristic curve.

ICD	Description	No. Positive	No. Negative	AUC
I. Certain infectious and parasitic diseases				
A04	Other bacterial intestinal infections	4538	203478	0.69
A07	Other protozoal intestinal diseases	77	207939	0.86
A17	Tuberculosis of nervous system	16	208000	0.66
A18	Tuberculosis of other organs	46	207970	0.69
A28	Other zoonotic bacterial diseases, not elsewhere classified	20	207996	0.80
A31	Infection due to other mycobacteria	622	207394	0.66
A37	Whooping cough	6	208010	0.70
A38	Scarlet fever	5	208011	0.75
A41	Other sepsis	9615	198401	0.72
A43	Nocardiosis	181	207835	0.69
A46	Erysipelas	57	207959	0.70
A49	Bacterial infection of unspecified site	4226	203790	0.66
A51	Early syphilis	39	207977	0.84
A56	Other sexually transmitted chlamydial diseases	10	208006	0.75
A58	Granuloma inguinale	1	208015	0.75
A59	Trichomoniasis	49	207967	0.82
A60	Anogenital herpesviral [herpes simplex] infections	638	207378	0.67
A64	Unspecified sexually transmitted disease	149	207867	0.68
A68	Relapsing fevers	41	207975	0.85
A74	Other diseases caused by chlamydiae	181	207835	0.84
A78	Q fever	1	208015	0.75
A81	Atypical virus infections of central nervous system	10	208006	0.78
A87	Viral meningitis	20	207996	0.72
A93	Other arthropod-borne viral fevers, not elsewhere classified	66	207950	0.69
B10	Other human herpesviruses	6	208010	0.66
B15	Acute hepatitis A	10	208006	0.68
B17	Other acute viral hepatitis	476	207540	0.69
B18	Chronic viral hepatitis	2877	205139	0.66
B25	Cytomegaloviral disease	1441	206575	0.70
B27	Infectious mononucleosis	242	207774	0.74
B34	Viral infection of unspecified site	4433	203583	0.66
B39	Histoplasmosis	17	207999	0.66
B44	Aspergillosis	1259	206757	0.72

Continued on next page

Table A1 – Continued from previous page

ICD	Description	No. Positive	No. Negative	AUC
B45	Cryptococcosis	97	207919	0.79
B46	Zygomycosis	42	207974	0.92
B49	Unspecified mycosis	2197	205819	0.71
B58	Toxoplasmosis	148	207868	0.72
B59	Pneumocystosis	277	207739	0.72
B71	Other cestode infections	4	208012	0.90
B89	Unspecified parasitic disease	3146	204870	0.66
B95	Streptococcus, Staphylococcus, and Enterococcus as the cause of diseases classified elsewhere	4023	203993	0.66
B99	Other and unspecified infectious diseases	3264	204752	0.66
II. Neoplasms				
C00	Malignant neoplasm of lip	15	208001	0.67
C01	Malignant neoplasm of base of tongue	336	207680	0.70
C07	Malignant neoplasm of parotid gland	115	207901	0.71
C10	Malignant neoplasm of oropharynx	762	207254	0.67
C12	Malignant neoplasm of pyriform sinus	59	207957	0.82
C13	Malignant neoplasm of hypopharynx	133	207883	0.76
C15	Malignant neoplasm of esophagus	1294	206722	0.86
C16	Malignant neoplasm of stomach	903	207113	0.74
C19	Malignant neoplasm of rectosigmoid junction	606	207410	0.76
C20	Malignant neoplasm of rectum	1300	206716	0.66
C22	Malignant neoplasm of liver and intrahepatic bile ducts	1543	206473	0.69
C24	Malignant neoplasm of other and unspecified parts of biliary tract	241	207775	0.75
C25	Malignant neoplasm of pancreas	1808	206208	0.67
C26	Malignant neoplasm of other and ill-defined digestive organs	36	207980	0.75
C30	Malignant neoplasm of nasal cavity and middle ear	91	207925	0.70
C31	Malignant neoplasm of accessory sinuses	111	207905	0.67
C33	Malignant neoplasm of trachea	56	207960	0.75
C34	Malignant neoplasm of bronchus and lung	7297	200719	0.65
C37	Malignant neoplasm of thymus	72	207944	0.67
C38	Malignant neoplasm of heart, mediastinum and pleura	438	207578	0.70
C40	Malignant neoplasm of bone and articular cartilage of limbs	151	207865	0.76
C41	Malignant neoplasm of bone and articular cartilage of other and unspecified sites	683	207333	0.84
C43	Malignant melanoma of skin	2715	205301	0.68
C44	Other and unspecified malignant neoplasm of skin	8754	199262	0.72
C45	Mesothelioma	471	207545	0.66

Continued on next page

Table A1 – Continued from previous page

ICD	Description	No. Positive	No. Negative	AUC
C47	Malignant neoplasm of peripheral nerves and autonomic nervous system	55	207961	0.77
C48	Malignant neoplasm of retroperitoneum and peritoneum	458	207558	0.71
C49	Malignant neoplasm of other connective and soft tissue	2172	205844	0.66
C4A	Merkel cell carcinoma	110	207906	0.70
C50	Malignant neoplasm of breast	6721	201295	0.71
C52	Malignant neoplasm of vagina	79	207937	0.78
C53	Malignant neoplasm of cervix uteri	374	207642	0.67
C54	Malignant neoplasm of corpus uteri	1394	206622	0.70
C56	Malignant neoplasm of ovary	1383	206633	0.81
C57	Malignant neoplasm of other and unspecified female genital organs	283	207733	0.72
C60	Malignant neoplasm of penis	37	207979	0.76
C61	Malignant neoplasm of prostate	7370	200646	0.74
C65	Malignant neoplasm of renal pelvis	234	207782	0.78
C66	Malignant neoplasm of ureter	300	207716	0.75
C67	Malignant neoplasm of bladder	2917	205099	0.68
C70	Malignant neoplasm of meninges	8	208008	0.73
C71	Malignant neoplasm of brain	1412	206604	0.68
C78	Secondary malignant neoplasm of respiratory and digestive organs	3679	204337	0.66
C81	Hodgkin lymphoma	1152	206864	0.66
C83	Non-follicular lymphoma	3445	204571	0.66
C85	Other specified and unspecified types of non-Hodgkin lymphoma	4594	203422	0.66
C88	Malignant immunoproliferative diseases and certain other B-cell lymphomas	640	207376	0.66
C90	Multiple myeloma and malignant plasma cell neoplasms	2495	205521	0.66
C91	Lymphoid leukemia	2874	205142	0.85
C92	Myeloid leukemia	3581	204435	0.71
C94	Other leukemias of specified cell type	340	207676	0.77
C95	Leukemia of unspecified cell type	1399	206617	0.79
D03	Melanoma in situ	623	207393	0.71
D04	Carcinoma in situ of skin	1390	206626	0.74
D05	Carcinoma in situ of breast	1071	206945	0.71
D06	Carcinoma in situ of cervix uteri	71	207945	0.75
D09	Carcinoma in situ of other and unspecified sites	519	207497	0.72
D11	Benign neoplasm of major salivary glands	131	207885	0.67
D18	Hemangioma and lymphangioma, any site	9065	198951	0.67
D21	Other benign neoplasms of connective and other soft tissue	843	207173	0.71
D22	Melanocytic nevi	18638	189378	0.65

Continued on next page

Table A1 – Continued from previous page

ICD	Description	No. Positive	No. Negative	AUC
D24	Benign neoplasm of breast	151	207865	0.68
D25	Leiomyoma of uterus	1037	206979	0.76
D29	Benign neoplasm of male genital organs	36	207980	0.70
D31	Benign neoplasm of eye and adnexa	1660	206356	0.68
D38	Neoplasm of uncertain behavior of middle ear and respiratory and intrathoracic organs	145	207871	0.71
D39	Neoplasm of uncertain behavior of female genital organs	68	207948	0.76
D41	Neoplasm of uncertain behavior of urinary organs	118	207898	0.70
D43	Neoplasm of uncertain behavior of brain and central nervous system	74	207942	0.65
D46	Myelodysplastic syndromes	2172	205844	0.69
D48	Neoplasm of uncertain behavior of other and unspecified sites	11434	196582	0.69
III. Diseases of the blood and blood-forming organs and certain disorders involving the immune mechanism				
D50	Iron deficiency anemia	22100	185916	0.83
D51	Vitamin B12 deficiency anemia	951	207065	0.69
D52	Folate deficiency anemia	127	207889	0.73
D53	Other nutritional anemias	1751	206265	0.66
D55	Anemia due to enzyme disorders	19	207997	0.77
D57	Sickle-cell disorders	764	207252	0.78
D58	Other hereditary hemolytic anemias	517	207499	0.67
D59	Acquired hemolytic anemia	637	207379	0.70
D61	Other aplastic anemias and other bone marrow failure syndromes	4953	203063	0.71
D62	Acute posthemorrhagic anemia	1870	206146	0.65
D63	Anemia in chronic diseases classified elsewhere	9162	198854	0.72
D64	Other anemias	37738	170278	0.74
D65	Disseminated intravascular coagulation [defibrination syndrome]	98	207918	0.73
D66	Hereditary factor VIII deficiency	48	207968	0.83
D70	Neutropenia	5568	202448	0.70
D71	Functional disorders of polymorphonuclear neutrophils	87	207929	0.68
D73	Diseases of spleen	1120	206896	0.73
D76	Other specified diseases with participation of lymphoreticular and reticuloendothelial tissue	56	207960	0.89
D80	Immunodeficiency with predominantly antibody defects	1965	206051	0.67
D84	Other immunodeficiencies	8544	199472	0.67
IV. Endocrine, nutritional and metabolic diseases				
E02	Subclinical iodine-deficiency hypothyroidism	81	207935	0.71

Continued on next page

Table A1 – Continued from previous page

ICD	Description	No. Positive	No. Negative	AUC
E08	Diabetes mellitus due to underlying condition	6980	201036	0.70
E09	Drug or chemical induced diabetes mellitus	2559	205457	0.70
E10	Type 1 diabetes mellitus	2752	205264	0.69
E11	Type 2 diabetes mellitus	39367	168649	0.70
E13	Other specified diabetes mellitus	10846	197170	0.71
E16	Other disorders of pancreatic internal secretion	4051	203965	0.68
E21	Hyperparathyroidism and other disorders of parathyroid gland	5167	202849	0.94
E24	Cushing's syndrome	294	207722	0.72
E26	Hyperaldosteronism	325	207691	0.69
E28	Ovarian dysfunction	1727	206289	0.78
E29	Testicular dysfunction	1529	206487	0.72
E30	Disorders of puberty, not elsewhere classified	23	207993	0.87
E32	Diseases of thymus	68	207948	0.75
E40	Kwashiorkor	218	207798	0.65
E43	Unspecified severe protein-calorie malnutrition	3645	204371	0.76
E44	Protein-calorie malnutrition of moderate and mild degree	2449	205567	0.70
E46	Unspecified protein-calorie malnutrition	4893	203123	0.71
E50	Vitamin A deficiency	278	207738	0.69
E51	Thiamine deficiency	194	207822	0.70
E53	Deficiency of other B group vitamins	6236	201780	0.81
E56	Other vitamin deficiencies	1935	206081	0.70
E59	Dietary selenium deficiency	16	208000	0.69
E60	Dietary zinc deficiency	343	207673	0.66
E63	Other nutritional deficiencies	1415	206601	0.71
E64	Sequelae of malnutrition and other nutritional deficiencies	32	207984	0.73
E65	Localized adiposity	321	207695	0.67
E66	Overweight and obesity	31279	176737	0.71
E72	Other disorders of amino-acid metabolism	290	207726	0.77
E76	Disorders of glycosaminoglycan metabolism	6	208010	0.89
E78	Disorders of lipoprotein metabolism and other lipidemias	80058	127958	0.71
E79	Disorders of purine and pyrimidine metabolism	1032	206984	0.75
E83	Disorders of mineral metabolism	16980	191036	0.88
E84	Cystic fibrosis	370	207646	0.77
E85	Amyloidosis	4061	203955	0.76
E87	Other disorders of fluid, electrolyte and acid-base balance	41520	166496	0.71
E95		677	207339	0.80
E96		6	208010	0.82
V. Mental and behavioural disorders				
F01	Vascular dementia	830	207186	0.75
F02	Dementia in other diseases classified elsewhere	2145	205871	0.70

Continued on next page

Table A1 – Continued from previous page

ICD	Description	No. Positive	No. Negative	AUC
F03	Unspecified dementia	2420	205596	0.72
F05	Delirium due to known physiological condition	850	207166	0.73
F10	Alcohol related disorders	10995	197021	0.67
F11	Opioid related disorders	7803	200213	0.69
F12	Cannabis related disorders	1256	206760	0.74
F13	Sedative, hypnotic, or anxiolytic related disorders	1121	206895	0.72
F14	Cocaine related disorders	1838	206178	0.70
F15	Other stimulant related disorders	791	207225	0.75
F16	Hallucinogen related disorders	61	207955	0.82
F18	Inhalant related disorders	4903	203113	0.73
F19	Other psychoactive substance related disorders	7052	200964	0.70
F25	Schizoaffective disorders	1055	206961	0.68
F28	Other psychotic disorder not due to a substance or known physiological condition	50	207966	0.70
F30	Manic episode	346	207670	0.69
F31	Bipolar disorder	4005	204011	0.66
F42	Obsessive-compulsive disorder	869	207147	0.66
F44	Dissociative and conversion disorders	825	207191	0.75
F45	Somatoform disorders	699	207317	0.65
F48	Other nonpsychotic mental disorders	1773	206243	0.66
F50	Eating disorders	2453	205563	0.71
F53	Mental and behavioral disorders associated with the puerperium, not elsewhere classified	149	207867	0.83
F55	Abuse of non-psychoactive substances	17	207999	0.68
F59	Unspecified behavioral syndromes associated with physiological disturbances and physical factors	4	208012	0.95
F60	Specific personality disorders	1096	206920	0.71
F63	Impulse disorders	2034	205982	0.66
F64	Gender identity disorders	129	207887	0.73
F68	Other disorders of adult personality and behavior	71	207945	0.66
F69	Unspecified disorder of adult personality and behavior	79	207937	0.65
F70	Mild intellectual disabilities	25	207991	0.72
F73	Profound intellectual disabilities	3	208013	0.88
F79	Unspecified intellectual disabilities	437	207579	0.71
F80	Specific developmental disorders of speech and language	313	207703	0.75
F81	Specific developmental disorders of scholastic skills	292	207724	0.66
F82	Specific developmental disorder of motor function	45	207971	0.87
F84	Pervasive developmental disorders	383	207633	0.73
F88	Other disorders of psychological development	38	207978	0.86

Continued on next page

Table A1 – Continued from previous page

ICD	Description	No. Positive	No. Negative	AUC
F89	Unspecified disorder of psychological development	58	207958	0.70
F90	Attention-deficit hyperactivity disorders	3730	204286	0.70
F93	Emotional disorders with onset specific to childhood	9	208007	0.82
F94	Disorders of social functioning with onset specific to childhood and adolescence	5	208011	0.79
F95	Tic disorder	80	207936	0.68
F98	Other behavioral and emotional disorders with onset usually occurring in childhood and adolescence	1063	206953	0.67
F99	Mental disorder, not otherwise specified	1694	206322	0.70
VI. Diseases of the nervous system				
G00	Bacterial meningitis, not elsewhere classified	16	208000	0.65
G01	Meningitis in bacterial diseases classified elsewhere	23	207993	0.73
G03	Meningitis due to other and unspecified causes	524	207492	0.66
G04	Encephalitis, myelitis and encephalomyelitis	712	207304	0.68
G08	Intracranial and intraspinal phlebitis and thrombophlebitis	486	207530	0.76
G09	Sequelae of inflammatory diseases of central nervous system	5	208011	0.67
G10	Huntington's disease	14	208002	0.80
G12	Spinal muscular atrophy and related syndromes	273	207743	0.71
G14	Postpolio syndrome	46	207970	0.69
G20	Parkinson's disease	1874	206142	0.76
G23	Other degenerative diseases of basal ganglia	265	207751	0.68
G30	Alzheimer's disease	1393	206623	0.71
G31	Other degenerative diseases of nervous system, not elsewhere classified	2970	205046	0.80
G37	Other demyelinating diseases of central nervous system	299	207717	0.69
G43	Migraine	9325	198691	0.76
G45	Transient cerebral ischemic attacks and related syndromes	5929	202087	0.75
G47	Sleep disorders	38056	169960	0.68
G53	Cranial nerve disorders in diseases classified elsewhere	9	208007	0.89
G59	Mononeuropathy in diseases classified elsewhere	11	208005	0.68
G63	Polyneuropathy in diseases classified elsewhere	949	207067	0.67
G65	Sequelae of inflammatory and toxic polyneuropathies	5	208011	0.72
G72	Other and unspecified myopathies	1360	206656	0.67

Continued on next page

Table A1 – Continued from previous page

ICD	Description	No. Positive	No. Negative	AUC
G73	Disorders of myoneural junction and muscle in diseases classified elsewhere	16	208000	0.66
G80	Cerebral palsy	188	207828	0.76
G82	Paraplegia (paraparesis) and quadriplegia (quadriparalysis)	1221	206795	0.71
G90	Disorders of autonomic nervous system	2506	205510	0.66
G99	Other disorders of nervous system in diseases classified elsewhere	763	207253	0.73
VII. Diseases of the eye and adnexa				
H01	Other inflammation of eyelid	4351	203665	0.67
H16	Keratitis	1645	206371	0.68
H17	Corneal scars and opacities	543	207473	0.68
H21	Other disorders of iris and ciliary body	647	207369	0.66
H25	Age-related cataract	20273	187743	0.69
H26	Other cataract	7856	200160	0.70
H27	Other disorders of lens	288	207728	0.80
H30	Chorioretinal inflammation	153	207863	0.70
H31	Other disorders of choroid	1296	206720	0.71
H32	Chorioretinal disorders in diseases classified elsewhere	6	208010	0.90
H34	Retinal vascular occlusions	2193	205823	0.69
H35	Other retinal disorders	12142	195874	0.68
H36	Retinal disorders in diseases classified elsewhere	82	207934	0.96
H40	Glaucoma	12452	195564	0.66
H42	Glaucoma in diseases classified elsewhere	20	207996	0.68
H43	Disorders of vitreous body	8807	199209	0.68
H46	Optic neuritis	740	207276	0.76
H61	Other disorders of external ear	9860	198156	0.67
H65	Nonsuppurative otitis media	1785	206231	0.66
H66	Suppurative and unspecified otitis media	1857	206159	0.69
H68	Eustachian salpingitis and obstruction	12	208004	0.69
H70	Mastoiditis and related conditions	157	207859	0.76
H71	Cholesteatoma of middle ear	191	207825	0.76
H74	Other disorders of middle ear mastoid	193	207823	0.69
H80	Otosclerosis	123	207893	0.68
H81	Disorders of vestibular function	4017	203999	0.78
H90	Conductive and sensorineural hearing loss	13695	194321	0.68
H91	Other and unspecified hearing loss	9658	198358	0.68
VIII. Diseases of the ear and mastoid process				
H73	Other disorders of tympanic membrane	140	359760	0.72
H90	Conductive and sensorineural hearing loss	5640	354260	0.71
H80	Otosclerosis	180	359720	0.69
H91	Other and unspecified hearing loss	4660	355240	0.68

Continued on next page

Table A1 – Continued from previous page

ICD	Description	No. Positive	No. Negative	AUC
H61	Other disorders of external ear	2360	357540	0.66
IX. Diseases of the circulatory system				
I01	Rheumatic fever with heart involvement	289	207727	0.71
I05	Rheumatic mitral valve diseases	5545	202471	0.88
I06	Rheumatic aortic valve diseases	959	207057	0.89
I07	Rheumatic tricuspid valve diseases	3259	204757	0.86
I08	Multiple valve diseases	559	207457	0.93
I09	Other rheumatic heart diseases	391	207625	0.93
I10	Essential (primary) hypertension	97583	110433	0.82
I11	Hypertensive heart disease	2816	205200	0.82
I12	Hypertensive chronic kidney disease	3195	204821	0.88
I13	Hypertensive heart and chronic kidney disease	2332	205684	0.76
I15	Secondary hypertension	8638	199378	0.77
I16	Hypertensive crisis	2772	205244	0.71
I20	Angina pectoris	26244	181772	0.72
I21	Acute myocardial infarction	20255	187761	0.95
I22	Subsequent ST elevation (STEMI) and non-ST elevation (NSTEMI) myocardial infarction	191	207825	0.69
I23	Certain current complications following ST elevation (STEMI) and non-ST elevation (NSTEMI) myocardial infarction (within the 28 day period)	288	207728	0.96
I24	Other acute ischemic heart diseases	6601	201415	0.81
I25	Chronic ischemic heart disease	54195	153821	0.76
I27	Other pulmonary heart diseases	11242	196774	0.71
I31	Other diseases of pericardium	11668	196348	0.71
I32	Pericarditis in diseases classified elsewhere	132	207884	0.73
I33	Acute and subacute endocarditis	6462	201554	0.78
I34	Nonrheumatic mitral valve disorders	13311	194705	0.88
I35	Nonrheumatic aortic valve disorders	18469	189547	0.91
I36	Nonrheumatic tricuspid valve disorders	3471	204545	0.91
I37	Nonrheumatic pulmonary valve disorders	812	207204	0.86
I38	Endocarditis, valve unspecified	5048	202968	0.90
I39	Endocarditis and heart valve disorders in diseases classified elsewhere	167	207849	0.81
I42	Cardiomyopathy	26650	181366	0.95
I43	Cardiomyopathy in diseases classified elsewhere	1881	206135	0.83
I44	Atrioventricular and left bundle-branch block	11488	196528	0.92
I45	Other conduction disorders	9159	198857	0.91
I46	Cardiac arrest	5423	202593	0.77
I47	Paroxysmal tachycardia	23608	184408	0.85
I48	Atrial fibrillation and flutter	55138	152878	0.95
I49	Other cardiac arrhythmias	71655	136361	0.71
I50	Heart failure	53172	154844	0.83
I60	Nontraumatic subarachnoid hemorrhage	1725	206291	0.70

Continued on next page

Table A1 – Continued from previous page

ICD	Description	No. Positive	No. Negative	AUC
I62	Other and unspecified nontraumatic intracranial hemorrhage	5100	202916	0.70
I63	Cerebral infarction	17773	190243	0.71
I65	Occlusion and stenosis of precerebral arteries, not resulting in cerebral infarction	8115	199901	0.72
I66	Occlusion and stenosis of cerebral arteries, not resulting in cerebral infarction	315	207701	0.73
I67	Other cerebrovascular diseases	9082	198934	0.73
I68	Cerebrovascular disorders in diseases classified elsewhere	308	207708	0.70
I69	Sequelae of cerebrovascular disease	2454	205562	0.76
I70	Atherosclerosis	9515	198501	0.70
I71	Aortic aneurysm and dissection	10134	197882	0.75
I73	Other peripheral vascular diseases	14279	193737	0.72
I74	Arterial embolism and thrombosis	2504	205512	0.75
I75	Atheroembolism	81	207935	0.67
I76	Septic arterial embolism	214	207802	0.75
I78	Diseases of capillaries	1055	206961	0.67
I79	Disorders of arteries, arterioles and capillaries in diseases classified elsewhere	3239	204777	0.77
I81	Portal vein thrombosis	603	207413	0.77
I82	Other venous embolism and thrombosis	16623	191393	0.79
I85	Esophageal varices	1375	206641	0.75
I96	Gangrene, not elsewhere classified	1818	206198	0.75
I97	Intraoperative and postprocedural complications and disorders of circulatory system, not elsewhere classified	1037	206979	0.82
X. Diseases of the respiratory system				
J00	Acute nasopharyngitis [common cold]	402	207614	0.76
J01	Acute sinusitis	5576	202440	0.65
J03	Acute tonsillitis	293	207723	0.72
J05	Acute obstructive laryngitis [croup] and epiglottitis	31	207985	0.67
J06	Acute upper respiratory infections of multiple and unspecified sites	13780	194236	0.69
J12	Viral pneumonia, not elsewhere classified	3581	204435	0.66
J14	Pneumonia due to <i>Hemophilus influenzae</i>	150	207866	0.75
J15	Bacterial pneumonia, not elsewhere classified	1983	206033	0.67
J16	Pneumonia due to other infectious organisms, not elsewhere classified	569	207447	0.74
J17	Pneumonia in diseases classified elsewhere	522	207494	0.77
J21	Acute bronchiolitis	642	207374	0.67
J30	Vasomotor and allergic rhinitis	10397	197619	0.75
J41	Simple and mucopurulent chronic bronchitis	2702	205314	0.69
J42	Unspecified chronic bronchitis	2812	205204	0.69

Continued on next page

Table A1 – Continued from previous page

ICD	Description	No. Positive	No. Negative	AUC
J43	Emphysema	7288	200728	0.72
J44	Other chronic obstructive pulmonary disease	14586	193430	0.77
J47	Bronchiectasis	2564	205452	0.65
J61	Pneumoconiosis due to asbestos and other mineral fibers	110	207906	0.73
J63	Pneumoconiosis due to other inorganic dusts	5	208011	0.77
J67	Hypersensitivity pneumonitis due to organic dust	201	207815	0.75
J69	Pneumonitis due to solids and liquids	3929	204087	0.66
J80	Acute respiratory distress syndrome	4105	203911	0.74
J81	Pulmonary edema	9663	198353	0.76
J82	Pulmonary eosinophilia, not elsewhere classified	103	207913	0.67
J84	Other interstitial pulmonary diseases	7742	200274	0.67
J85	Abscess of lung and mediastinum	444	207572	0.76
J86	Pyothorax	1127	206889	0.74
J90	Pleural effusion, not elsewhere classified	12465	195551	0.70
J91	Pleural effusion in conditions classified elsewhere	12341	195675	0.70
J92	Pleural plaque	301	207715	0.69
J93	Pneumothorax and air leak	1276	206740	0.68
J95	Intraoperative and postprocedural complications and disorders of respiratory system, not elsewhere classified	2636	205380	0.70
J96	Respiratory failure, not elsewhere classified	17510	190506	0.74
XI. Diseases of the digestive system				
K01	Embedded and impacted teeth	482	207534	0.66
K04	Diseases of pulp and periapical tissues	2466	205550	0.70
K06	Other disorders of gingiva and edentulous alveolar ridge	372	207644	0.65
K20	Esophagitis	4515	203501	0.66
K22	Other diseases of esophagus	6132	201884	0.67
K23	Disorders of esophagus in diseases classified elsewhere	4	208012	0.98
K26	Duodenal ulcer	687	207329	0.70
K28	Gastrojejunal ulcer	610	207406	0.71
K40	Inguinal hernia	3585	204431	0.70
K44	Diaphragmatic hernia	2484	205532	0.67
K46	Unspecified abdominal hernia	898	207118	0.67
K50	Crohn's disease	1898	206118	0.81
K65	Peritonitis	2788	205228	0.66
K67	Disorders of peritoneum in infectious diseases classified elsewhere	13	208003	0.96
K70	Alcoholic liver disease	2726	205290	0.74
K71	Toxic liver disease	374	207642	0.68
K72	Hepatic failure, not elsewhere classified	1642	206374	0.76
K74	Fibrosis and cirrhosis of liver	4888	203128	0.71

Continued on next page

Table A1 – Continued from previous page

ICD	Description	No. Positive	No. Negative	AUC
K83	Other diseases of biliary tract	3251	204765	0.66
K85	Acute pancreatitis	4293	203723	0.66
K90	Intestinal malabsorption	2428	205588	0.83
K91	Intraoperative and postprocedural complications and disorders of digestive system, not elsewhere classified	1772	206244	0.65
K92	Other diseases of digestive system	18141	189875	0.66
K94	Complications of artificial openings of the digestive system	2136	205880	0.70
K95	Complications of bariatric procedures			
XII. Diseases of the skin and subcutaneous tissue				
L11	Other acantholytic disorders	400	207616	0.73
L12	Pemphigoid	171	207845	0.90
L22	Diaper dermatitis	53	207963	0.67
L27	Dermatitis due to substances taken internally	2264	205752	0.68
L42	Pityriasis rosea	32	207984	0.68
L43	Lichen planus	573	207443	0.69
L52	Erythema nodosum	66	207950	0.69
L57	Skin changes due to chronic exposure to non-ionizing radiation	16715	191301	0.70
L59	Other disorders of skin and subcutaneous tissue related to radiation	200	207816	0.67
L60	Nail disorders	9636	198380	0.66
L62	Nail disorders in diseases classified elsewhere	1	208015	0.86
L65	Other nonscarring hair loss	3892	204124	0.66
L68	Hypertrichosis	350	207666	0.65
L70	Acne	2870	205146	0.66
L71	Rosacea	3160	204856	0.67
L73	Other follicular disorders	3652	204364	0.72
L82	Seborrheic keratosis	19887	188129	0.69
L83	Acanthosis nigricans	134	207882	0.69
L84	Corns and callosities	4061	203955	0.70
L87	Transepidermal elimination disorders	3	208013	0.66
L89	Pressure ulcer	4029	203987	0.69
L94	Other localized connective tissue disorders	862	207154	0.67
L97	Non-pressure chronic ulcer of lower limb, not elsewhere classified	6677	201339	0.72
XIII. Diseases of the musculoskeletal system and connective tissue				
M01	Direct infections of joint in infectious and parasitic diseases classified elsewhere	164	207852	0.92
M07	Enteropathic arthropathies	29	207987	0.77
M08	Juvenile arthritis	61	207955	0.68
M10	Gout	8135	199881	0.78
M11	Other crystal arthropathies	1152	206864	0.68

Continued on next page

Table A1 – Continued from previous page

ICD	Description	No. Positive	No. Negative	AUC
M12	Other and unspecified arthropathy	13209	194807	0.65
M14	Arthropathies in other diseases classified elsewhere	448	207568	0.72
M15	Polyosteoarthritis	5637	202379	0.69
M16	Osteoarthritis of hip	6221	201795	0.66
M17	Osteoarthritis of knee	13448	194568	0.69
M18	Osteoarthritis of first carpometacarpal joint	1806	206210	0.67
M19	Other and unspecified osteoarthritis	17952	190064	0.66
M1A	Chronic gout	4508	203508	0.74
M22	Disorder of patella	848	207168	0.72
M24	Other specific joint derangements	1681	206335	0.69
M32	Systemic lupus erythematosus (SLE)	1676	206340	0.65
M33	Dermatopolymyositis	450	207566	0.78
M34	Systemic sclerosis [scleroderma]	627	207389	0.72
M36	Systemic disorders of connective tissue in diseases classified elsewhere	24	207992	0.75
M40	Kyphosis and lordosis	651	207365	0.70
M48	Other spondylopathies	12891	195125	0.66
M61	Calcification and ossification of muscle	34	207982	0.71
M66	Spontaneous rupture of synovium and tendon	303	207713	0.67
M80	Osteoporosis with current pathological fracture	3189	204827	0.69
M81	Osteoporosis without current pathological fracture	12985	195031	0.70
M83	Adult osteomalacia	80	207936	0.80
M85	Other disorders of bone density and structure	10859	197157	0.67
M86	Osteomyelitis	4033	203983	0.67
M88	Osteitis deformans [Paget's disease of bone]	61	207955	0.77
M89	Other disorders of bone	14272	193744	0.79
M97	Periprosthetic fracture around internal prosthetic joint	389	207627	0.74
XIV. Diseases of the genitourinary system				
N00	Acute nephritic syndrome	7	208009	0.91
N01	Rapidly progressive nephritic syndrome	41	207975	0.81
N02	Recurrent and persistent hematuria	370	207646	0.80
N03	Chronic nephritic syndrome	116	207900	0.85
N04	Nephrotic syndrome	716	207300	0.71
N05	Unspecified nephritic syndrome	1322	206694	0.85
N06	Isolated proteinuria with specified morphological lesion	478	207538	0.68
N07	Hereditary nephropathy, not elsewhere classified	8	208008	0.93
N08	Glomerular disorders in diseases classified elsewhere	4897	203119	0.75
N10	Acute pyelonephritis	1131	206885	0.70
N11	Chronic tubulo-interstitial nephritis	30	207986	0.70

Continued on next page

Table A1 – Continued from previous page

ICD	Description	No. Positive	No. Negative	AUC
N12	Tubulo-interstitial nephritis, not specified as acute or chronic	3491	204525	0.67
N14	Drug- and heavy-metal-induced tubulo-interstitial and tubular conditions	147	207869	0.90
N15	Other renal tubulo-interstitial diseases	123	207893	0.70
N17	Acute kidney failure	29637	178379	0.70
N18	Chronic kidney disease (CKD)	35840	172176	0.77
N19	Unspecified kidney failure	1978	206038	0.82
N21	Calculus of lower urinary tract	598	207418	0.65
N25	Disorders resulting from impaired renal tubular function	3173	204843	0.71
N29	Other disorders of kidney and ureter in diseases classified elsewhere	37	207979	0.67
N31	Neuromuscular dysfunction of bladder, not elsewhere classified	3342	204674	0.75
N33	Bladder disorders in diseases classified elsewhere	5	208011	0.79
N35	Urethral stricture	430	207586	0.88
N40	Benign prostatic hyperplasia	14094	193922	0.85
N41	Inflammatory diseases of prostate	1115	206901	0.69
N42	Other and unspecified disorders of prostate	436	207580	0.67
N43	Hydrocele and spermatocele	495	207521	0.71
N45	Orchitis and epididymitis	655	207361	0.66
N46	Male infertility	235	207781	0.73
N47	Disorders of prepuce	759	207257	0.71
N48	Other disorders of penis	1496	206520	0.68
N49	Inflammatory disorders of male genital organs, not elsewhere classified	341	207675	0.67
N50	Other and unspecified disorders of male genital organs	2481	205535	0.67
N52	Male erectile dysfunction	6547	201469	0.71
N60	Benign mammary dysplasia	966	207050	0.71
N61	Inflammatory disorders of breast	529	207487	0.68
N63	Unspecified lump in breast	3650	204366	0.65
N64	Other disorders of breast	4596	203420	0.67
N65	Deformity and disproportion of reconstructed breast	18	207998	0.87
N70	Salpingitis and oophoritis	177	207839	0.71
N71	Inflammatory disease of uterus, except cervix	282	207734	0.82
N73	Other female pelvic inflammatory diseases	311	207705	0.74
N75	Diseases of Bartholin's gland	92	207924	0.75
N76	Other inflammation of vagina and vulva	2934	205082	0.73
N77	Vulvovaginal ulceration and inflammation in diseases classified elsewhere	6	208010	0.72
N80	Endometriosis	862	207154	0.82

Continued on next page

Table A1 – Continued from previous page

ICD	Description	No. Positive	No. Negative	AUC
N81	Female genital prolapse	1933	206083	0.72
N82	Fistulæ involving female genital tract	361	207655	0.71
N83	Noninflammatory disorders of ovary, fallopian tube and broad ligament	2586	205430	0.74
N84	Polyp of female genital tract	566	207450	0.71
N85	Other noninflammatory disorders of uterus, except cervix	674	207342	0.71
N87	Dysplasia of cervix uteri	379	207637	0.74
N88	Other noninflammatory disorders of cervix uteri	450	207566	0.67
N89	Other noninflammatory disorders of vagina	5529	202487	0.70
N90	Other noninflammatory disorders of vulva and perineum	1579	206437	0.68
N91	Absent, scanty and rare menstruation	1476	206540	0.80
N92	Excessive, frequent and irregular menstruation	2918	205098	0.80
N93	Other abnormal uterine and vaginal bleeding	3578	204438	0.73
N94	Pain and other conditions associated with female genital organs and menstrual cycle	3583	204433	0.72
N95	Menopausal and other perimenopausal disorders	7587	200429	0.71
N96	Recurrent pregnancy loss	149	207867	0.79
N97	Female infertility	808	207208	0.83
N98	Complications associated with artificial fertilization	21	207995	0.93
XV. Pregnancy, childbirth and the puerperium				
O00	Ectopic pregnancy	55	207961	0.89
O02	Other abnormal products of conception	150	207866	0.84
O03	Spontaneous abortion	241	207775	0.89
O08	Complications following ectopic and molar pregnancy	1	208015	0.84
O09	Supervision of high risk pregnancy	2019	205997	0.85
O10	Pre-existing hypertension complicating pregnancy, childbirth and the puerperium	194	207822	0.67
O11	Pre-existing hypertension with pre-eclampsia	21	207995	0.81
O12	Gestational [pregnancy-induced] edema and proteinuria without hypertension	61	207955	0.90
O13	Gestational [pregnancy-induced] hypertension without significant proteinuria	297	207719	0.82
O14	Pre-eclampsia	353	207663	0.85
O15	Eclampsia	104	207912	0.85
O16	Unspecified maternal hypertension	507	207509	0.80
O20	Hemorrhage in early pregnancy	303	207713	0.84
O21	Excessive vomiting in pregnancy	395	207621	0.84
O22	Venous complications and hemorrhoids in pregnancy	533	207483	0.66
O23	Infections of genitourinary tract in pregnancy	165	207851	0.82

Continued on next page

Table A1 – Continued from previous page

ICD	Description	No. Positive	No. Negative	AUC
O24	Diabetes mellitus in pregnancy, childbirth, and the puerperium	495	207521	0.83
O25	Malnutrition in pregnancy, childbirth and the puerperium	96	207920	0.90
O26	Maternal care for other conditions predominantly related to pregnancy	766	207250	0.89
O28	Abnormal findings on antenatal screening of mother	291	207725	0.74
O30	Multiple gestation	99	207917	0.89
O32	Maternal care for malpresentation of fetus	84	207932	0.91
O34	Maternal care for abnormality of pelvic organs	206	207810	0.87
O35	Maternal care for known or suspected fetal abnormality and damage	191	207825	0.78
O36	Maternal care for other fetal problems	965	207051	0.86
O40	Polyhydramnios	48	207968	0.92
O41	Other disorders of amniotic fluid and membranes	172	207844	0.78
O42	Premature rupture of membranes	52	207964	0.82
O43	Placental disorders	29	207987	0.90
O44	Placenta previa	141	207875	0.88
O45	Premature separation of placenta [abruptio placentae]	15	208001	0.81
O46	Antepartum hemorrhage, not elsewhere classified	221	207795	0.82
O47	False labor	80	207936	0.79
O48	Late pregnancy	51	207965	0.88
O60	Preterm labor	63	207953	0.91
O69	Labor and delivery complicated by umbilical cord complications	8	208008	0.82
O70	Perineal laceration during delivery	13	208003	0.93
O71	Other obstetric trauma	7	208009	0.89
O72	Postpartum hemorrhage	47	207969	0.87
O73	Retained placenta and membranes, without hemorrhage	20	207996	0.89
O76	Abnormality in fetal heart rate and rhythm complicating labor and delivery	33	207983	0.71
O80	Encounter for full-term uncomplicated delivery	692	207324	0.88
O82	Encounter for cesarean delivery without indication	611	207405	0.83
O85	Puerperal sepsis	94	207922	0.67
O86	Other puerperal infections	131	207885	0.68
O87	Venous complications and hemorrhoids in the puerperium	5	208011	0.79
O88	Obstetric embolism	35	207981	0.82
O89	Complications of anesthesia during the puerperium	1	208015	0.92

Continued on next page

Table A1 – Continued from previous page

ICD	Description	No. Positive	No. Negative	AUC
O90	Complications of the puerperium, not elsewhere classified	264	207752	0.72
O91	Infections of breast associated with pregnancy, the puerperium and lactation	20	207996	0.84
O92	Other disorders of breast and disorders of lactation associated with pregnancy and the puerperium	62	207954	0.88
O98	Maternal infectious and parasitic diseases classifiable elsewhere but complicating pregnancy, childbirth and the puerperium	235	207781	0.86
O99	Other maternal diseases classifiable elsewhere but complicating pregnancy, childbirth and the puerperium	1245	206771	0.85
O9A	Maternal malignant neoplasms, traumatic injuries and abuse classifiable elsewhere but complicating pregnancy, childbirth and the puerperium	10	208006	0.93
P00	Newborn affected by maternal conditions that may be unrelated to present pregnancy	5	208011	0.97
P01	Newborn affected by maternal complications of pregnancy	3	208013	0.93
P02	Newborn affected by complications of placenta, cord and membranes	3	208013	0.85
P03	Newborn affected by other complications of labor and delivery	2	208014	0.75
P04	Newborn affected by noxious substances transmitted via placenta or breast milk	42	207974	0.69
P05	Disorders of newborn related to slow fetal growth and fetal malnutrition	56	207960	0.66
P07	Disorders of newborn related to short gestation and low birth weight, not elsewhere classified	55	207961	0.91
P08	Disorders of newborn related to long gestation and high birth weight	11	208005	0.87
P09	Abnormal findings on neonatal screening	43	207973	0.88
P12	Birth injury to scalp	28	207988	0.72
P22	Respiratory distress of newborn	3	208013	0.99
P24	Neonatal aspiration	72	207944	0.73
P27	Chronic respiratory disease originating in the perinatal period	33	207983	0.87
P28	Other respiratory conditions originating in the perinatal period	10	208006	0.89
P29	Cardiovascular disorders originating in the perinatal period	113	207903	0.75
P36	Bacterial sepsis of newborn	1	208015	1.00

Continued on next page

Table A1 – Continued from previous page

ICD	Description	No. Positive	No. Negative	AUC
P37	Other congenital infectious and parasitic diseases	2	208014	0.87
P38	Omphalitis of newborn	50	207966	0.90
P52	Intracranial nontraumatic hemorrhage of newborn	1	208015	0.95
P59	Neonatal jaundice from other and unspecified causes	10	208006	0.99
P61	Other perinatal hematological disorders	4	208012	1.00
P70	Transitory disorders of carbohydrate metabolism specific to newborn	3	208013	1.00
P74	Other transitory neonatal electrolyte and metabolic disturbances	20	207996	0.69
P77	Necrotizing enterocolitis of newborn	1	208015	1.00
P78	Other perinatal digestive system disorders	11	208005	0.99
P81	Other disturbances of temperature regulation of newborn	4	208012	0.99
P83	Other conditions of integument specific to newborn	47	207969	0.87
P90	Convulsions of newborn	12	208004	0.96
P91	Other disturbances of cerebral status of newborn	18	207998	0.90
P92	Feeding problems of newborn	53	207963	0.99
P94	Disorders of muscle tone of newborn	4	208012	0.97
P95	Stillbirth	2	208014	0.71
P96	Other conditions originating in the perinatal period	34	207982	0.90